



Analytical tools for cyclodextrin nanosponges in pharmaceutical field: a review

Sunil Kumar¹ · Rekha Rao¹

Received: 13 January 2019 / Accepted: 21 March 2019 / Published online: 1 April 2019
© Springer Nature B.V. 2019

Abstract

With the growing popularity of the nanomedicine-based pharmaceutical market, active molecules from chemical and natural origin are encapsulated in various nanocarriers enhancing their therapeutic efficacy. Depending upon the fabricated functionality, cyclodextrin based nanosponges has become a potential vehicle to encapsulate the active molecules. To explore nanosponges-based delivery system in pharmacy, knowledge of the analytical tools that could significantly assess their quality parameters, has major role for researchers working in this field. Owing to understand their benefits and potential toxicity, characteristic features like safety, negligible toxicity, superior inclusion capability, marked swelling behaviour and biodegradability are the primarily basis for their use in drug delivery, drug targeting, tissue engineering and regenerative medicine. This review article focuses on the various aspects of analytical techniques applied for characterization of nanosponges, which may affect quality of these nanocarriers. Subsequently, the challenges for characterization of these systems have been especially emphasized. In addition, sincere efforts have been made to compile various analytical techniques for description and understanding of these nanostructures from existing literature. Recommendations and suggestions are also mentioned while selecting suitable analytic techniques to characterize the quality parameters of nanosponges.

Keywords Porous particles · Analytical technique · Microscopy · Spectroscopy · Thermal analysis · Zeta potential

Introduction

Recent advances in the nanotechnology evidence the increasing attention towards the supramolecular fabrication of drugs for therapeutic and pharmaceutical applications. The fabrication of the baby biomaterials with nanosized structural features can be anticipated to cater challenges associated with drug delivery. A variety of nanomedicines have been explored including nanosuspensions, nanolipid carriers, nanoemulsions, nanotubes among which, nanosponges (NS) have appealed the researchers and obtained a tremendous impetus, as they possess many advantages for drug delivery including improvement in stability, solubility and appearance. Their small size results in large surface area leading to enhanced absorption and permeation through membranes. Also, these nanocarriers allow controlled

release of entrapped molecules and drug targeting via tagging with specific linkers [1, 2]. Additionally, the nanosponges are self sterile and highly insoluble in water as well as organic solvents. They can remain stable up to 300 °C and from pH 2–11. Encapsulation of wide array of molecules like hydrophobic, hydrophilic and immiscible liquids offers a high potential to these nanosystems [2–5].

Nanosponges are hyper-cross linked colloidal structures composed of polymer and crosslinker, possessing numerous cavities in which drug moieties can be entrapped. Although, variety of polymers can be used for crosslinking but β -cyclodextrins (CD) have been most commonly explored in these nanosystems. Further, crosslinking can also be tailored for desired release rate requirements and wide drug loading capacity by varying ratio of CD and cross linker. For this, cross linkers like hexamethylene diisocyanate (HMDI), carbonyl diimidazole (CDI), pyromellitic dianhydride (PMDA), diphenyl carbonate (DPC) could be employed [2]. The structural representation of these cross linkers and β -cyclodextrin is represented in Fig. 1.

A number of patents filed for nanosponges signify its growing importance in drug delivery nowadays. ‘cyclodextrin

✉ Rekha Rao
rekhaline@gmail.com

¹ Department of Pharmaceutical Sciences, Guru Jambheshwar University of Science and Technology, Hisar, Haryana 125001, India

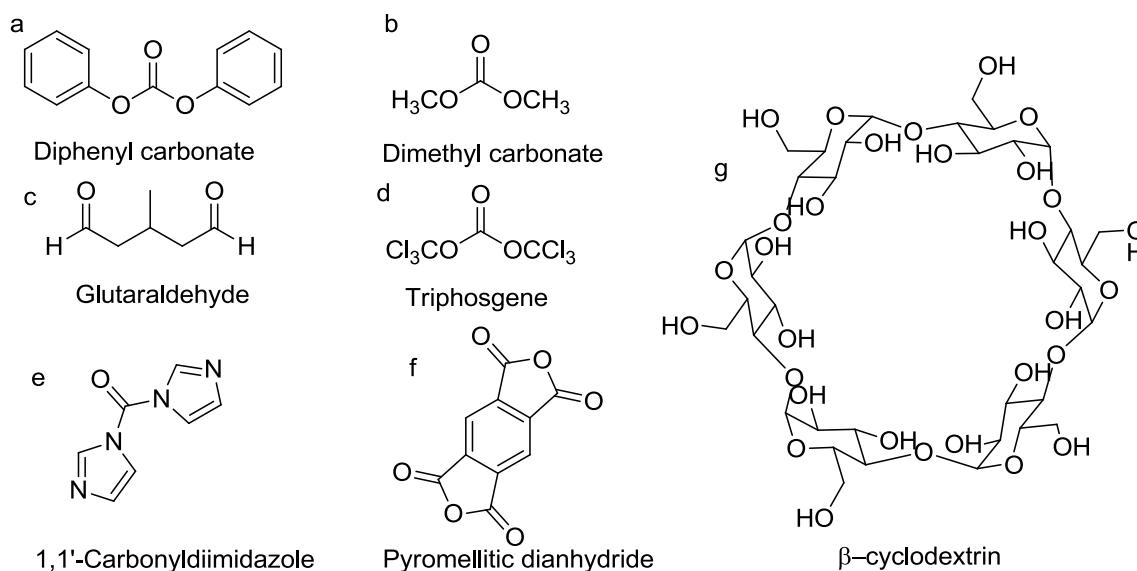


Fig. 1 Various cross-linkers (a–f) and β -cyclodextrin (g) used in fabrication of cyclodextrin nanosponges

nanosponges' term was originally owned by Minn Ma and De Quan Li in 1998 [6]. Trotta and his research group formulated cyclodextrin NS using carbonates as crosslinkers by ultrasound-assisted synthesis [7]. Following this, Trotta and co-workers invented the hyper cross-linked nanoporous complexes for antitumor drugs like camptothecin, paclitaxel, tamoxifen, docetaxel and their derivatives [8]. Later on, Trotta et al, patented a novel method of preparation of dextrin NS [9].

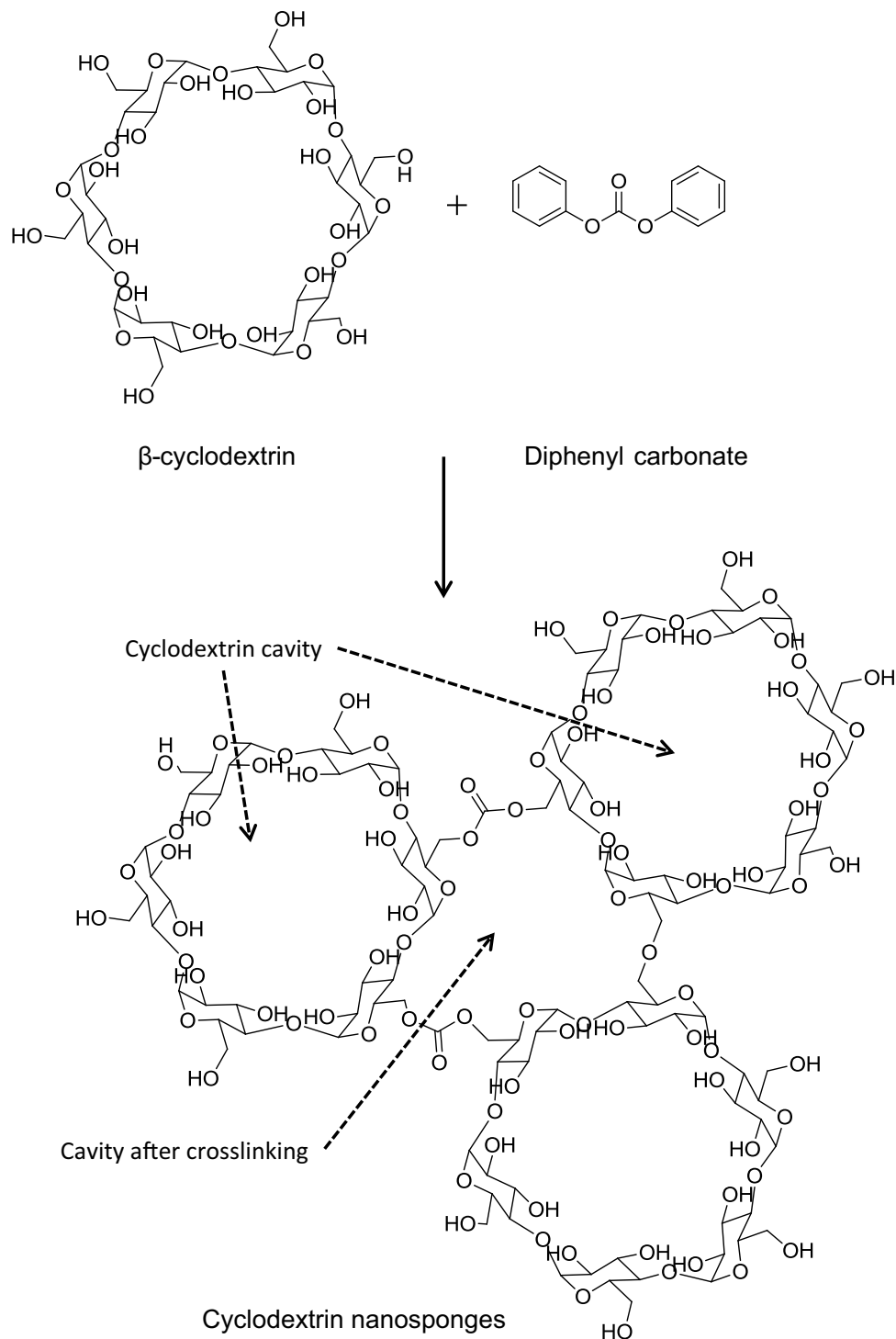
The nanosponges can be fabricated through various techniques namely ultrasound-assisted synthesis [10], solvent evaporation technique [11], melt method [12, 13], emulsion solvent diffusion method [14] and microwave assisted synthesis [15]. The schematic representation of fabrication of blank nanosponges is shown in Fig. 2. Further, it is noteworthy that NS have been reported safe due to the biodegradable nature of the cyclodextrins, with minimum in vitro and in vivo toxicity [16]. Shende and his research group fabricated the β -cyclodextrin based NS, and carried out acute and repeated (oral) dose toxicity studies in Wistar rats. The best tolerated dose for all prepared NS formulations was found to be 2000 mg/kg [17]. In vitro evaluation carried out on cell lines such as HaCaT, HELA, COS, Vero, MCF7, HCPC-1, HT-29 have advocated that cyclodextrin nanosponges possess no cytotoxicity [13, 18]. Further, it was proved that incubation of these nanosystems with erythrocytes for approximately ninety minutes did not induce any haemolytic modifications [18].

The general description of the cyclodextrin nanosponges (CD-NS) have been discussed in various reviews [2, 5]. Tejashri et al, explored the features of CD-NS and their application in the arena of pharmaceutical

sciences [19]. Chilajwar et al, exploited the application of the CD-NS as new realm of the nanotechnology [18]. Recently, Shere et al, published a critical review on cyclodextrin based nanosponges [20]. Nevertheless, in spite of wide literature on NS, only a single review has been recently reported on characterization of the dynamic and structural features of the CD-NS [21]. A thorough physicochemical characterization of NS is of critical importance, representing a crucial step in order to explore the best potential advantages of these systems. To study the interaction of loaded drugs with NS and to empathize the process of their fabrication, synthesis and design, characterization of NS through suitable analytical techniques is need of the hour. Full analytical characterization of NS can assist in selection of most appropriate polymer, crosslinker as well as increase the pharmaceutical applications of these systems along with possible implications of patenting and commercialization.

However, complete characterization of NS is a great challenge, owing to their peculiar physicochemical properties. For characterization of these nanocarriers viz. spectroscopic techniques like Ultraviolet/visible (UV–Vis) spectrophotometry, nuclear magnetic resonance (NMR), Raman spectroscopy, Fourier transform infrared (FTIR), thermal analysis via Differential scanning calorimetry (DSC) and Thermogravimetric analysis (TGA), X-ray diffraction (XRD), microscopy techniques including confocal laser scanning microscopy (CLSM), atomic force microscopy (AFM), transmission electron microscopy (TEM), scanning electron microscopy (SEM), zeta sizer have been reported which help in substantiating the formation of these systems as shown in Fig. 3 [2, 4, 22].

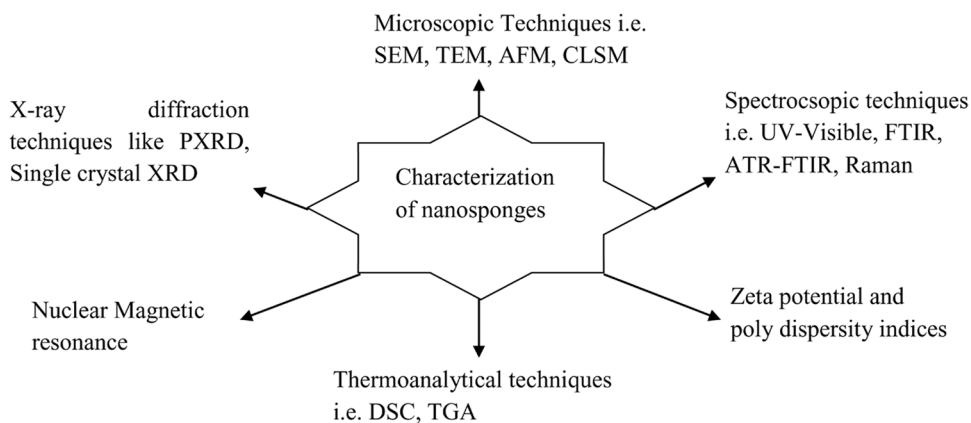
Fig. 2 Schematic representation of fabrication of blank nanosponges



The purpose of this review is to explore the major analytical tools for complete characterization of cyclodextrin nanosponges, in powder (solid), liquid and semi-solid states, with their corresponding possible merits and

drawbacks. Further, the applicability of every investigated tool is elaborated by relevant previous research reports. To narrow the focus of present review, we have considered

Fig. 3 Analytical techniques used in evaluation of nano-sponges



the analytical approaches for cyclodextrin nanosponges particularly related to pharmaceutical application.

Analytical techniques to characterize nanosponges

The assessment of the formation of nanosponges and their complete characterization is not a straightforward assignment and require employment of various sophisticated analytical methods in order to explore their features. The concomitant use of different analytical techniques would facilitate a better interpretation of host–guest interactions and further, assist in appropriate selection of suitable polymer structures for available guest representing pharmaceutical active moiety. The variation in physical or chemical properties of the active moieties encapsulated in NS, can also be detected by different analytical techniques. Further, these techniques enable to determine experimental variations in NS with more precision and accuracy. The major analytical tools reported in literature for the characterization of NS include spectroscopy, microscopy, thermal analysis, diffractometry, zeta potential and nuclear magnetic resonance. Here, in this review, a number of major tools that can be implemented or has already been implemented for NS characterization and evaluation have been described in detail.

Spectroscopic approaches

The spectroscopic approaches symbolise a worthwhile integral tool to recognise and evaluate the hyper cross-linked polymer structures, nanosponges. Upon NS formation, variation in properties like absorbance, wave number, NMR shift, and fluorescence intensity of the system can be measured by various spectroscopic methods.

Ultraviolet–visible spectrophotometry

In an effort to optimize and analysis of nanosponges in solution, UV–Visible spectrophotometry is a simple, fast, economic and valuable method. Encapsulation in NS give rises to a substantial change in the absorption spectrum of the guest leading to band broadening or bathochromic shift. Depending upon drug chromophore position, the shift of guest moiety from an aqueous medium to the channels of the NS can alter its master copy of UV–Visible absorption spectrum [23]. The UV–Visible spectrum of the active moiety modified in the form of NS may ascertain the encapsulation of drug in these polymeric structures. However, due to the presence of interfering moieties, this technique lags specificity. Hence, it does not provide a significant evidence of the formation of drug loaded NS. As a result of NS formation, the changes in the bathochromic or hypsochromic shifts of the maximum absorption of active moiety, increase or decrease in intensity of UV–Visible spectrum may be seen [23]. The solubilisation efficiency of various active moieties like telmisartan [24], acetyl salicylic acid [25], resveratrol [26], repaglinide [27], quercetin [28], efavirenz [12], babchi oil [13] encapsulated in NS have been analysed using UV–Visible spectrophotometer at $\lambda_{\text{max}} = 296, 234, 303, 283, 372, 286, 265$ nm, respectively.

Anandam and Selvamuthukumar carried out determination of drug loading, in vitro release, simulated intestinal fluid stability assay, metal chelating activity and photostability studies for quercetin NS using UV–Visible spectrophotometer ($\lambda_{\text{max}} = 372$ nm). Whereas in the same work, 1,1-diphenyl-2-picrylhydrazyl hydrate (DPPH) scavenging activity, superoxide anion-scavenging activity assay and anti-superoxide formation assay were also assessed spectrophotometrically at $\lambda_{\text{max}} = 517, 550, 295$ nm, respectively [28].

The interaction of the paclitaxel with nanosponges has been studied using UV–Visible spectroscopy [29]. In order to measure entrapment efficiency and in vitro release profile, the analysis of econazole nitrate in different solvents like

methanol, phosphate buffer (pH 6.8 and 7.4) was carried out at $\lambda_{\text{max}} = 271, 266$ and 272 nm, respectively [14].

Fourier-transform infrared spectroscopy

FTIR is a widely used tool for characterization of nanosponges. Generally, FTIR absorption measurements are implemented on dried samples, in range $600\text{--}4000$ cm^{-1} at room temperature [5]. During the cross-linking, the vibrational modes of the polymers, cross-linkers and active molecule gets shifted from original positions leading to broadening or disappearance of the characteristic bands of the active moiety, cross-linker, and polymer. Fluctuation in peak intensity and displacement in their wave number may also take place indicating interaction of polymers either with itself or with cross-linker. The restriction of the stretching vibration in these molecules induced by cross-linking between polymer, cross-linker and drug, may lead to these changes. Additionally, inter atomic bond weakening takes place upon cross-linking and/or complexation in NS. Besides significant selectivity and sensitivity, other chief advantages of this analytical technique include affordable cost, extensive diffusion, rapid and easy acquisition time of spectrum. Sample preparation for FTIR investigation represents a conceivable limitation. Mixing powder (sample) and potassium bromide and converting matrix into transparent pellet are the primary steps to carry out FTIR analysis. Moreover, fluctuation in mixing and dimensions of prepared pellets lower its usefulness for quantitative estimations. Further, hygroscopic nature of potassium bromide may also lead to physicochemical changes in sample. Another possible limitation includes frequent masking or overlapping of the characteristic peaks of the active moiety by the polymer or cross-linker bands [30, 31].

In FTIR spectra of the blank nanosponges, peak ranging from 1700 to 1750 cm^{-1} confirms the presence of the carbonate bond. However, the starting material for nanosponge synthesis, β -cyclodextrin shows no peak in the above mentioned range of FTIR spectrum [15]. Cavalli and co-workers confirmed the presence of carbonate bond at 1700 cm^{-1} in nanosponge structures through FTIR [32].

The camptothecin have prominent characteristic peaks at around $1750, 1460\text{--}1600, 1270\text{--}1290$ cm^{-1} , which shifted or broadened in nanosponges elucidating prominent interactions between active molecule and nano formulations [33].

Darandale and Vavia compared curcumin nanosponges (CrNS), blank nanosponges and pure curcumin spectra as shown in Fig. 4. Plain nanosponges with major band of carbonate bond ($1720\text{--}1750$ cm^{-1}) ascertained cyclodextrin-based nanosponge formation. Moreover, the other distinguishing peaks of nanosponges have been observed at 2918 cm^{-1} , 1418 cm^{-1} and 1026 cm^{-1} due to the C–H stretching vibration, C–H bending vibration and

C–O stretching vibration of primary alcohol, respectively. The prominent peaks of pure curcumin were observed at about 3503 cm^{-1} , 1508 cm^{-1} , 1427 cm^{-1} , 1273 cm^{-1} and $1026/856$ cm^{-1} corresponding to phenolic O–H stretching, the C=O and C=C vibration, olefinic C–H bending vibration, aromatic C–O stretching vibration, and C–O–C stretching of the curcumin, respectively. The acute absorption peak (1605 cm^{-1}) corresponding to benzene ring (stretching vibrations), were also depicted in curcumin FTIR spectrum. In curcumin loaded nanosponges, similar peaks as that of plain nanosponges along with some major curcumin peaks were observed. The peak shifting to higher or lower wave number viz. $1026\text{--}1029$ cm^{-1} , $1418\text{--}1409$ cm^{-1} , $1745\text{--}1749$ cm^{-1} and $2918\text{--}2914$ cm^{-1} confirmed the curcumin complexation with nanosponges in these formulations [11].

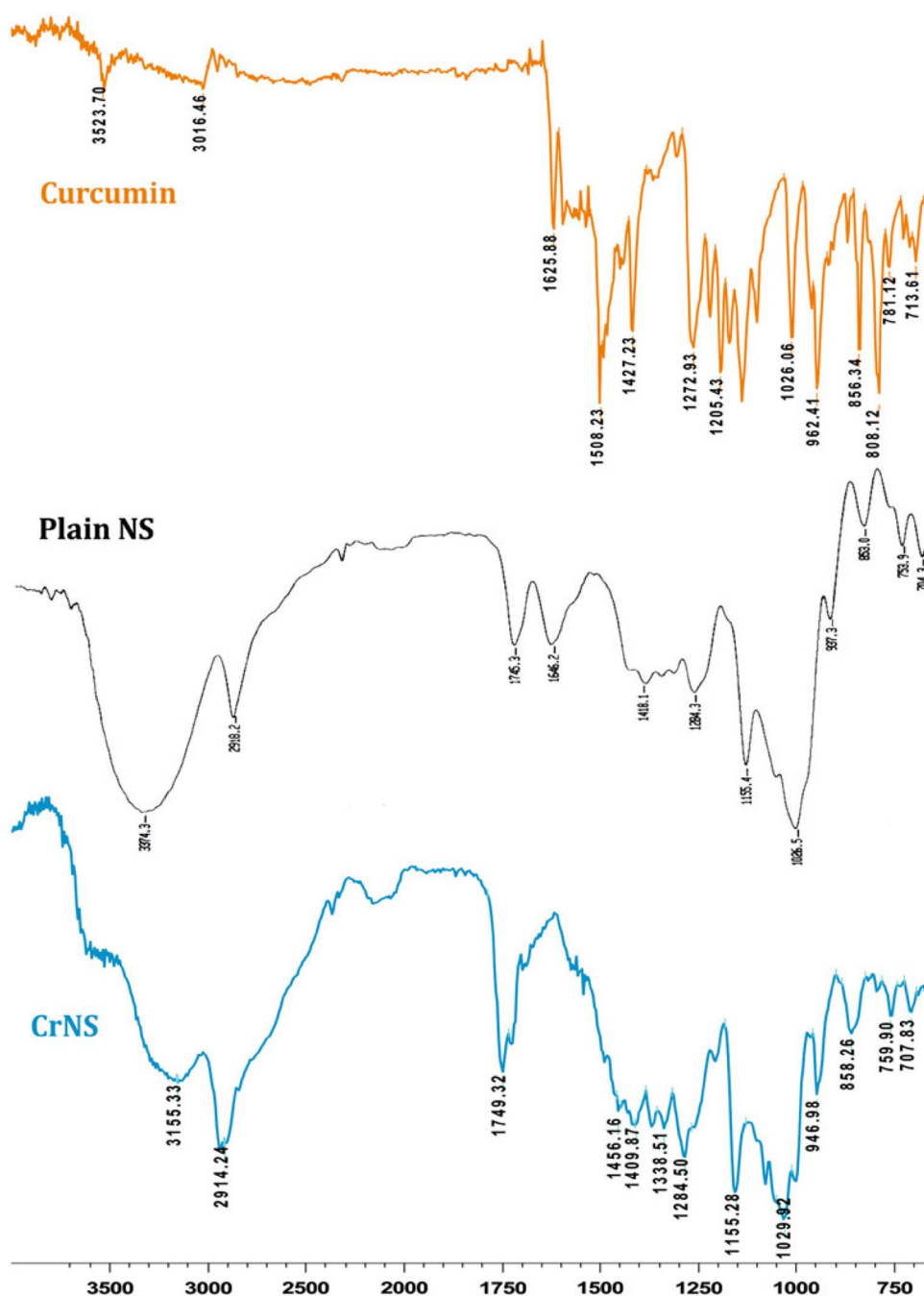
According to Rao and coworkers, telmisartan showed the characteristic peaks at $1350\text{--}1000, 1381, 1455, 1695, 3673$ cm^{-1} . The prominent peak of carbonyl group was observed at $1700\text{--}1703$ cm^{-1} in nanosponges while peak at 1700 cm^{-1} was absent in β -cyclodextrin FTIR spectrum. Weak interaction between nanosponges and telmisartan was confirmed from disappearing and broadening of few peaks. Upon addition of sodium bicarbonate, the frequency of C=O band has been reduced and O–H broad band was found disappeared in FTIR spectra of telmisartan. From above results, it was ascertained that sodium bicarbonate modulated the micro environmental pH as well as altered the drug crystalline nature to amorphous through molecular interactions resulting in enhanced dissolution of the active moiety [26].

FTIR spectra of blank nanosponges have intense band of carbonate bond ($1740\text{--}1750$ cm^{-1}), evidenced the fabrication of cyclodextrin NS. Peaks at 2918 cm^{-1} corresponding to the C–H stretching, 1418 cm^{-1} corresponding to C–H bending, and 1026 cm^{-1} corresponding to C–O stretching of primary alcohol, further supported this. A major change in finger print region ($900\text{--}1400$ cm^{-1}) was also observed on comparison of FTIR of quercetin and its nanosponge complex. The quercetin has intense peaks at $820\text{--}940, 1167, 1203, 1265, 1318, 1383, 1608, \text{ and } 1663$ cm^{-1} , which shifted/broadened in NS, indicating complexation of quercetin and nanosponges [28]. Numerous investigations utilizing FTIR as characterization tool for resveratrol [24], acetyl salicylic acid [25], acyclovir [34], telmisartan [26], is reported in various papers.

Attenuated total reflectance-FTIR spectroscopy

Attenuated total reflectance (ATR) setup in FTIR analytical technique works on the principle of complete reflection, when an infra red radiation crosses a convenient prism (made up of high refractive index infrared transmitting material). The powdered sample, placed on ATR crystal

Fig. 4 FTIR spectra of curcumin, plain NS and CrNS. Reprinted by permission from Springer Nature Customer Service Centre GmbH: Springer Nature, Journal of Inclusion Phenomena, Cyclodextrin-based nanosponges of curcumin: formulation and physicochemical characterization. Darandale, S.S., Vavia, P.R., copyright (2013)



(complete reflecting surface), is compressed with diamond piston to obtain clear sample layer in ATR measurements. In these arrangements, impermanent wave weakened in IR zone and sample ingests energy. Exponential reduction in intensity with length occurs from ATR crystal. Generally, the sample thickness does not affect ATR measurements. The sample preparation is not required; hence, counteract all limitations arising due to dispersion of sample in potassium bromide pellets. This is major advantage of ATR spectroscopy over the traditional FTIR analytical technique. In addition to this, absence of sample handling ascertains the higher

reproducibility and rapidity, making this technique suitable in observing variations in solid forms, like hydrated or polymorphic forms [35]. Generally, ATR-FTIR absorption measurements are carried out on dried samples in 400–4000 cm^{-1} wave number range with temperature extending from 250 to 320 K. It is a reproducible non-destructive technique, requiring minimum amount (μg) of sample. Additionally, chemical analysis can be carried out instantly on ATR spectra, averting complicated calculations. Spectra displays very good signal-to-noise ratio resulting in avoidance of bands saturation [36].

A number of publications describing ATR-FTIR measurements of drugs/bio actives loaded nanosponges have been reported. Swaminathan and his research group carried out ATR-FTIR of dexamethasone and its NS in order to understand interactions between them. About $+40\text{ cm}^{-1}$ band transfer for C=O bond at 1780.05 cm^{-1} was observed in the crystalline type NS. The major peaks of dexamethasone ($1720, 1700, 1600, 1050$ and 900 cm^{-1}) were found widened with complex formation. Although, significant interactions of drug with crystalline as well as paracrystalline NS have been reported from ATR-FTIR studies, but researchers found sensitivity of this tool not acceptable to distinguish interactions in crystalline and paracrystalline NS. Therefore, DSC, TGA and Raman spectroscopy have also been performed in this study [10].

Apple polyphenols (chlorogenic acid, phloridzin and rutin) have been entrapped in CD-NS in order to enhance their stability at high temperature and in the presence of light. For confirmation of encapsulation of bioactives in NS, ATR-FTIR technique has been employed. The prominent peaks of rutin were observed at 1653 and 1596 cm^{-1} , corresponding to C=O stretching (C=O of ring C) and C=C stretching (aromatic ring), respectively. In addition to this, a peak at 1743 cm^{-1} was seen due to carbonate bond of carbonyl group between β -cyclodextrin and cross linker in NS and one another less prominent peak at 1632 cm^{-1} relating to O–H moiety deformation was there. In NS, a similar peak as in rutin was observed but at a lower frequency, 1639 cm^{-1} whereas peak at 1743 cm^{-1} remained unchanged. The intensity of band at 1630 – 1640 cm^{-1} was enhanced in the presence of rutin, due to input of two absorption bands from polyphenol. Similar results were found for phloridzin and chlorogenic acid. In case of phloridzin, two peaks were obtained at 1623 and 1604 cm^{-1} due to C=O stretching in a ketone group and C–C stretching in aromatic ring, respectively. However, the phloridzin-NS complex having molar ratio 1:4 displayed a wide peak at 1630 cm^{-1} and 1742 cm^{-1} . The chlorogenic acid spectrum presented three peaks at $1685, 1638$ and 1600 cm^{-1} corresponding to C=O stretching in carboxylic and ketone group, and C=C stretching in aromatic ring, respectively. Moreover, in its complex with NS, a peak appeared at 1634 cm^{-1} as discussed above for CD complex [37].

In a similar study, the ATR-FTIR was employed, along with DSC and powder X-ray diffraction (PXRD) analysis, to ascertain the fabrication of repaglinide loaded NS. Comparison of spectra of drug loaded NS with spectra of pure substances and physical mixtures helps in ascertaining the significant differences. The prominent O–H stretching vibration in 3300 – 3500 cm^{-1} region, and more prominent –CH and –CH₂– group vibrations in 2800 – 3300 cm^{-1} region which were significant for cyclodextrin, appear in NS spectra, too. The absorption peak of the repaglinide at 1684 cm^{-1} related

to C=O group and 3293.12 cm^{-1} related to N–H stretching were seen in repaglinide-sulfobutylether- β -cyclodextrin-NS and physical mixture while found absent in spectra of lyophilized complex. The disappearance of these peaks was due to host–guest interactions, indicating the drug encapsulation in the NS cavities [27].

In another study, Castiglione and co-workers elucidated the role of macrocycle size on the gel-to-sol evolution of CD-NS through ATR-FTIR geometry. This particular study was dedicated to detailed investigations using above mentioned analytical technique [38]. FTIR frequencies of the active molecules loaded with NS are enumerated in Table 1.

Raman spectroscopy

Raman spectroscopy is based on concept of the light scattering [57]. The interaction of light with matter results in various optical phenomena like absorption, transmission and scattering. The light-matter interaction is taken as collision (elastic or inelastic) on molecular level. In inelastic one, energy changes take place, named as Raman scattering whereas no energy transformations take place and scattered photon are distinguished at similar frequency as incident photon called Rayleigh scattering.

Raman spectra are presented through the wave number deviations from incident photons to scattered ones in contrast to scattering intensity. Upon radiation of material with laser light, the pattern of wavelength shifts are chief for a particular chemical fingerprint corresponding to molecular structure [58]. This molecular approach provides a valuable analytical method for identification and investigation of vibrational modes of molecules as well as for measuring modifications in molecular bonds. When compared to FTIR spectroscopy, this technique possesses some leading assists like no or little sample formation and insensitivity to water absorption bands [59]. Recently, it has greater utilizations in the pharmaceuticals and suggested as a useful analytical method for study of drug encapsulation in NS [60]. Not only this, Raman spectroscopy can be used in conjunction to FTIR to provide a better picture for understanding the drug and NS interactions. For the first time, Swaminathan and co-workers carried out the Raman spectroscopy to examine the interaction of dexamethasone and NS. On complexation with NS, the characteristic marker peaks of the dexamethasone at $680, 950, 1440, 1480$ and 1620 cm^{-1} in Raman spectroscopy of the pure drug were displaced or masked substantially, confirming the complexation [10]. In a similar study, the quercetin and quercetin loaded nanosponges were subjected to Raman spectroscopy to study the encapsulation and/or interactions. In this study, comparison of Raman spectra of quercetin, and quercetin NS has been shown. The marker peaks of quercetin were observed at $675, 1102, 1270, 1336, 1440, 1570$ and 1634 cm^{-1} in Raman spectra of pure

Table 1 Nanosponge analysis by FTIR as per literature reports

Sr. no.	Drug	Frequency (cm ⁻¹)	Remarks	References
1.	Camptothecin	1750, 1460–1600 and 1270–1290	Peaks broadened/disappeared	[33]
2.	Resveratrol	3273	O–H stretching in drug loaded NS	[24]
3.	Paclitaxel	3300, 1700	Reducing in O–H stretching reduced, and Aryl and saturated group confirmed interaction	[29]
4.	Acetyl salicylic acid	1756 and 1685	Acetoxyl carbonyl stretching and hydrogen bonded carboxyl carbonyl stretching	[25]
5.	Telmisartan	3673, 1695, 1455, 1381–1000	C=O band decreased and O–H broad band disappeared on addition of NaHCO ₃	[26]
6.	Dexamethasone	1780.05	Slight peak shifting (+ 40) for C=O bond of crystalline NS	[10]
7.	Curcumin	3503, 1605, 1508, 1427, 1273 and 1026/856	Upon complexation shifting of wave number (higher/lower) taken into account	[11]
8.	Acyclovir	1200–1600	Modified peaks proved interaction between drug and NS	[34]
9.	Repaglinide	3293.12, 1684	N–H stretching vibration and C=O	[27]
10.	Quercetin	1663, 1608, 1383, 1318, 1265, 1203, 1167 and 820–940	Peaks shifted or broadened on complexation	[28]
11.	Apple polyphenols (rutin)	1653, 1596	C=O and C=C stretching; Intensity increased upon complexation	[37]
12.	Apple polyphenols (Chlorogenic acid)	1685, 1638 and 1600	C=O stretching of carboxyl and ketone group; C=C stretching in aromatic ring	[37]
13.	Apple polyphenols (phloridzin)	1623, 1605	C=O stretching of ketone group; C=C stretching in aromatic ring; Increased intensity proved complexation	[37]
14.	Gabapentin	3631, 3480, 1536	Amino, carboxyl hydroxyl and cyclohexyl group stretching	[39]
15.	Meloxicam	1347, 1530, 1620, 2930, 3293.79	–S=O, aromatic C–C, –N–H, C–H aliphatic, and –S–N–; Shifted –C–C–, –C–H peaks confirms entrapment	[40]
16.	Melatonin	3327, 2893, 1060, 1740	Peak shifting confirmed presence of NS on substrate	[41]
17.	Lysozyme	1084, 878, 1455, 713, 1430	Symmetric stretching, symmetric bending, asymmetric stretching, asymmetric bending	[42]
18.	Levodopa	–	Thermal stability	[43]
19.	Quercetin	1663, 1608, 1383, 1318, 1265, 1203, 1167, 820–940	Shifting of these peaks confirms the interactions of drug with NS	[44]
20.	Efavirenz	3312, 2248, 1741.43 1496	N–H, C–H, C=O, C–F stretching, respectively	[12]
21.	Chrysin	3400–3500, 1665–1710, 1400–1500, 1000–1200	Broadening of peaks at these wave numbers evidenced the true interaction	[45]
22.	Rilpivirine HCl	1750, 2925, 1298, 1029	Carbonate, C–H, C–O	[46]
23.	DB103 (2-(3,4-dimethoxyphenyl)-3-phenyl-4H-pyrido[1,2-a]pyrimidin-4-one)	1657, 1511, 1463, 1260, 1015	C=O, C=N, CH ₃ , C–O–C asymmetric and symmetric stretching	[47]
24.	Norfloxacin	1720, 1606,	COOH and pyridine keto stretching	[48]
25.	Curcumin	3504, 1625, 1597, 1502, 1424, 1270, 1022/855	Phenolic O–H, C=O, benzene ring, C=O, C=C, olefinic, C–H, aromatic C–O, C–O–C	[49]

Table 1 (continued)

Sr. no.	Drug	Frequency (cm ⁻¹)	Remarks	References
26.	Doxorubicin	3380, 1737, 1757, 2868, 1660	OH, C=O, conjugated carbonyl ester, C–H	[50]
27.	Rilpivir	2216.58, 1198, 757.75, 1629.48, 1594.18, 1649	C=N, C–N, C–H, C=C, N–H, ester group; confirms complexation	[51]
28.	Strigolactones (MEB55 and ST362)	1780, 2900	C=O bond in D ring and C–H stretching	[52]
29.	Ellagic acid	–	–	[53]
30.	Atorvastatin calcium	1650, 1560, 1516, 3370, 3252, 3055	C=O, aromatic C=C, carboxylate, N–H stretching	[54]
31.	Rosuvastatin	3320, 2933, 1597, 1541, 1377, 1332, 1149,	O–H, C–H, C=C, COO ⁻ asymmetric and symmetric stretching, sulfone asymmetric and symmetric stretching	[55]
32.	Salvia officinalis essential oil	3417, 1938, 1642–1597	=C–H, C=O, C=C	[56]

drug. These characteristic peaks were found substantially displaced or masked in the drug loaded NS, confirming the complexation of the quercetin with NS [28].

In another investigation, Cruoi et al., presented a detailed inspection of the vibrational dynamics of CD-NS hydrogel in different states (gel or liquid suspension) by Raman spectroscopy to clarify the role of H-bond dynamics of water molecules in the nanopores of NS in order to determine their rigidity and maximum water holding capacity. Raman spectroscopy formed the sole basis of probing hydrogen bond dynamics of water in CD-NS hydrogel in detail [60]. The characteristic Raman peaks of drugs loaded with NS is depicted in Table 2.

In the following year, Rossi and her research group explored the molecular dynamics of polymeric matrix and water in pyromellitic anhydride-nanosponge hydrogel using the UV Raman scattering measurements. The modifications of the vibrational dynamics of the CD-NS hydrogel were examined by calculating the polymer hydration levels in water and NS matrix [61].

Nuclear magnetic resonance

Over the last few years, a variety of the state of the art approaches have been presented and found a widespread application in both academic and pharmaceutical research [62]. NMR is based on the principle of absorption of radiofrequency radiation by atomic nuclei with non zero spins

in a strong magnetic field [63]. The atomic nuclei absorption is affected by besieging atoms, causing small local alteration in the external magnetic field. In this, complete facts relating to molecular structure of the pharmacologically active sample can be accessed. The non-destructive, detection of different nuclei, structure sensitive, structural examination of samples in solution phase and solid phase include the important characteristics of NMR, allowing differentiation between molecules or portion of molecules with variable mobility. NMR analytical technique is generally beneficial to study the confirmation and structure of the macromolecules in pharmaceuticals.

NMR has been used to detect impurity of the drug quantitatively [64], quantify the active moieties in the biological fluids and pharmaceutical formulations, and characterization of the drug products [65, 66].

There are not many reports for use of NMR in nanosponges characterization. For the first time in 2014, Olteanu and co-workers carried out the physicochemical characterization of NS using ¹H NMR. The major changes in the chemical shift values from 0.47 to 0.24 ppm of protons of repaglinide A ring were measured in the ¹H NMR spectra of the repaglinide loaded β-cyclodextrin NS and sulfobutyl-ether-β-cyclodextrin NS. This confirmed the interaction of drug with both types of NS. It was expected that inclusion in the cyclodextrin hydrophobic cavities as well as steric hindrance due to β-cyclodextrin substitution have been found responsible for these interactions [27].

Table 2 Nanosponge analysis by Raman spectroscopy as per literature

Sr. no.	Active molecules	Characteristic Raman peaks	References
1.	Dexamethasone	680, 950, 1440, 1480 and 1620 cm ⁻¹	[10]
2.	Quercetin	675, 1102, 1270, 1336, 1440, 1570 and 1634 cm ⁻¹	[28]
3.	DS103	1600, 1330 and 650 cm ⁻¹	[47]

To measure the transport properties of the ibuprofen sodium loaded CD-NS, high resolution magic angle spinning NMR spectroscopy have been reported [67].

In order to characterize CD-NS fabricated using DPC and PMDA crosslinkers, predicted ^{13}C NMR spectra of these nanosponges presented a peak at 155.13 ppm corresponding to carbonyl carbon that cross-links β -cyclodextrin with DPC and peak at 168.57 and 168.60 ppm corresponding to ester carbonyl carbon which confirm the cross-linking of primary and secondary OH groups of β -cyclodextrin with PMDA. Moreover, the peak at 167.61 ppm represented to the carboxylic acid carbonyl carbon of the cross-linked β -cyclodextrins [49].

This technique possessed the potential to exploit the rational design of NS for drug targeting and delivery. As NMR is a valuable analytical technique to study the NS, it is expected that future studies on this drug delivery carrier should include evaluation using this technique as well.

Thermal analytical approaches

These analytical approaches commonly include DSC and TGA, and are crucial for catering fundamental data for the characterization of nanosponges. Owing to their simplicity, relative rapidity and reliability, DSC and TGA are widespread analytical approaches to solid-state characterization of multi component systems, including nanosponges.

Differential scanning calorimetry

It is a thermoanalytical tool used for measuring the alteration in chemical or physical properties of nanocarriers and their designing materials corresponding to change in temperature. The comparison of heat flow rate of the polymers, crosslinkers and active molecule and their nanosponges upon heating or cooling at same rate, is the measuring principle of DSC. Evolution or absorption of heat leads to variation in the differential heat flow, which are recorded as peaks. The peak area is generally directly proportional to the enthalpy change. Thermal events (both endothermic and exothermic) are generally confirmed by the direction of peak [68]. DSC is a precise and modern analytical method, to determine melting and decomposition point. Using this technique has chances of detecting an extra phase transition besides the melting point, considerably due to solid-to-solid phase transition and liquid crystal intermediates [69].

DSC has a pronounced impact on material science through the measurement of numerous physical and chemical properties of compounds. This technique elucidates the endothermic and exothermic processes at temperature range from -120 to 600 °C [70–74]. DSC allows to measure quantitative heat of transitions and reaction. It

differentiates first order thermodynamic variations such as fusion, and second order thermodynamic variations such as glass transition temperature, T_g [75]. Table 3 describes the thermal behaviour of the drug entrapped in the nanosponges.

The exhaustive cease of active moiety melting peak in DSC curve of NS is generally pretended as a confirmatory witness of encapsulation of active moiety inside NS cavity [76]. This may be due to transformation of crystalline moiety to amorphous form which may be the result of fabrication of inclusion composite [77]. Other evidences for ascertaining NS formation reported by researchers include changes in shape and temperature of CD peak, along with disappearance of drug melting peak and appearance of new peaks [78].

In case of nanosponges, the DSC instrument is generally calibrated with indium for heat of fusion and melting point. A heating rate of 5 or 10 °C per min is applied in the temperature range 30–450 °C under nitrogen purge. An empty pan is employed as reference standard [28, 40].

Sunder illustrated that the flexibility (T_g) of a modified extremely polar hyperbranched polymer (having prominent number of OH end groups) is ascertained chiefly by two factors using DSC analysis. One is ability of substituents to form highly branched phases viz. crystallization, mesophases. Another one includes the hydrogen bonding of terminal groups, enhancing the rigidity of the molecules [79]. The degree of alkyl substitution has a prominent effect on T_g and has barely effect on melting temperature (T_m) [79, 80].

Cavalli et al., encapsulated dexamethasone (lipophilic), flurbiprofen (lipophilic), doxorubicin hydrochloride (hydrophilic) in β -CDNS. The DSC thermograms of NS displayed no peak before 320 °C, showing high thermal stability. The NS-drug interaction was ascertained by absence of drug's melting peak. Further, it was speculated that molecular dispersion of drug in NS occurs in the CD hydrophobic pits for lipophilic actives, whereas hydrophilic actives partially or completely entrapped in the surrounding network [32].

Itraconazole NS were characterized using DSC in addition to XRD and photon correlation spectroscopy (PCS). In case of drug ternary composite, endotherm presented deviation of 10.74 °C in comparison to plain moiety whereas binary complex of drug NS displayed deviation of 6.48 °C. Similarly, itraconazole NS binary physical mixture presented deviation of a bare 0.5 °C and endotherm of ternary physical blend displayed deviation of 2.3 °C. These results indicated more complexation in drug ternary complex than NS. In addition to this, the endotherm and enthalpy area were found decreased in ternary composite than that of binary ones. The area and enthalpies of itraconazole observed the following order: plain moiety > moiety NS physical mixture > moiety NS solid dispersion > ternary physical blend > ternary solid dispersion, due to conversion of crystalline drug to

Table 3 Nanosponge characterization by DSC

Sr. no.	Active molecule	Temperature (°C)	Thermal behaviour	References
1.	Dexamethasone, flurbiprofen, doxorubicin hydrochloride	–	–	[32]
2.	Itraconazole	169	Endothermic	[81]
3.	Camptothecin	–	–	[33]
4.	Resveratrol	276	Exothermic	[24]
5.	Econazole nitrate	165	Exothermic	[14]
6.	Paclitaxel	216	Endothermic	[29]
7.	Acetyl salicylic acid	138	Endothermic	[25]
8.	Gamma-Oryzanol	167	Endothermic	[82]
9.	Dexamethasone	–	Endothermic	[10]
10.	Curcumin	176	Endothermic	[11]
11.	Acyclovir	260	Endothermic	[34]
12.	Telmisartan	269	Endothermic	[26]
13.	Rutin, phloridzin, chlorogenic acid	157, 118, 212	Endothermic	[37]
14.	Quercetin	318	Endothermic	[28, 44]
15.	Meloxicam	250	Endothermic	[40]
16.	Gabapentin	173.52	Endothermic	[39]
17.	Efavirenz	141	Endothermic	[12]
18.	Levodopa	310	–	[43]
19.	Lysozyme	73.8	Endothermic	[42]
20.	Melatonin	118	–	[41]
21.	Chrysin	290	Exothermic	[45]
22.	DB103	165 and 175	Double endothermic	[47]
23.	Rilpivirine HCl	242	Endothermic	[46]
24.	Atorvastatin Calcium	105–125 and 159.3	Endothermic	[54]
25.	Cholesterol	178–180	Endothermic	[50]
26.	Curcumin	185	Endothermic	[49]
27.	Norfloxacin	223.85 and 209.73	Endothermic	[48]
28.	Rilpivirine	243	Endothermic	[51]
29.	Rosuvastatin	225	Endothermic	[55]

amorphous form. Hence, the energy needed to melt the drug was decreased as enthalpy is reduced [81].

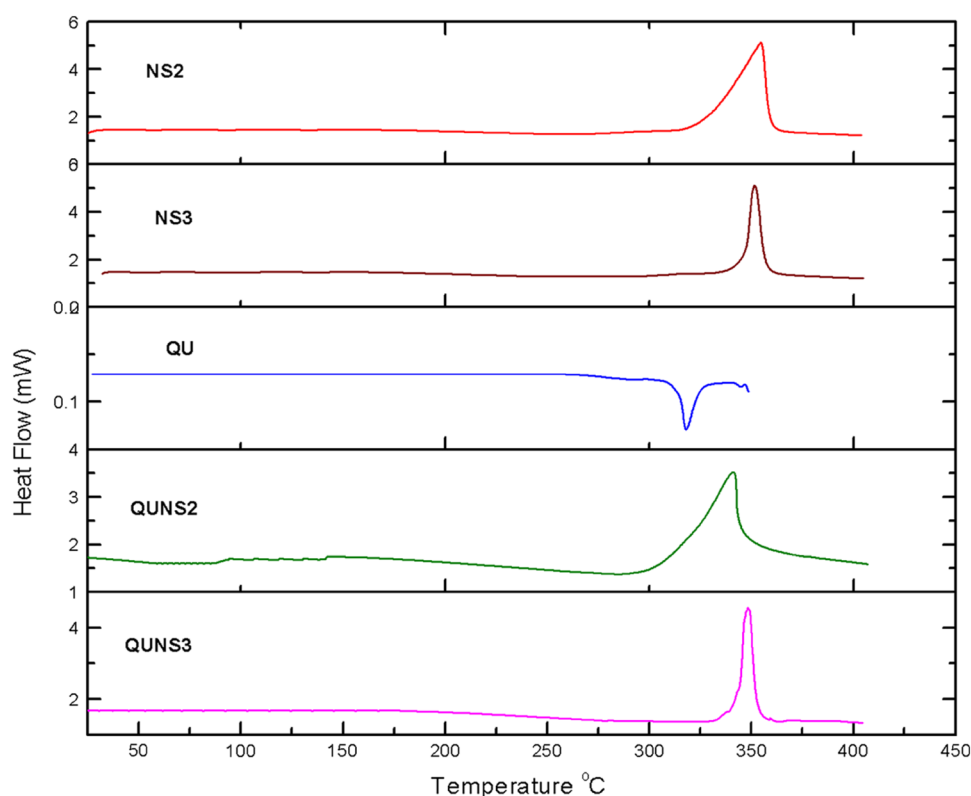
Acyclovir presented the endothermic peak at around 260 °C relating to the drug fusion. This endothermic peak disappeared in the endotherm of acyclovir loaded NS and drug loaded carboxylated NS indicating the molecular dispersion of acyclovir in these nanostructures. In contrast, acyclovir peak is present in the physical mixture (drug and NS) endotherm [34].

Differential scanning calorimetry analysis was performed in order to measure heat enthalpy of the individual polyphenols (chlorogenic acid, rutin and phloridzin), NS and polyphenol-NS composite. Rutin- 1, 1'-carbonyldiimidazole (1:8) complex thermogram presented an endothermic peak (157 °C), followed by one more peak (185 °C) for rutin which is in accordance with rutin melting point (195 °C). Pure NS, when became anhydrous displayed wide peak at 93 °C. Physical mixture curve was a combination of guest (rutin) compound and host (NS). Nevertheless, in NS

complex curve, the prominent peak of rutin disappeared, indicating the interaction between the host cavity and guest molecule. Similarly, for the phloridzin-1, 1'-carbonyldiimidazole (1:8) complexes, the same analysis was performed. Pure phloridzin melting point was observed at 118 °C, as an endothermic peak. Physical mixture of phloridzin and NS thermogram illustrated the presence of wide peak at 93 °C and a peak at 117 °C related to NS and phloridzin, respectively. The peak at 103 °C ascertained inclusion complex formation. Lastly, in the case of chlorogenic acid, the melting peak was presented around 212 °C. Its physical mixture curve displayed a broader endothermic peak (93 °C) and a narrow peak (211 °C) corresponding to NS and chlorogenic acid, respectively. Furthermore, the curve of NS evidenced the inclusion of guest (chlorogenic acid) into (host) NS cavity as shown from wide peak (94 °C) [37].

Evidence of NS complex formation has been provided by DSC thermograms for quercetin, plain NS, and quercetin-loaded NS complexes as shown in Fig. 5. The

Fig. 5 DSC thermograms of plain nanosponges (NS2 and NS3), pure quercetin (QU) and quercetin-loaded nanosponge complexes (QUNS2 and QUNS3). Reprinted by permission from Springer Nature Customer Service Centre GmbH: Springer Nature, *Journal of Materials Science, Fabrication of cyclodextrin nanosponges for quercetin delivery: physicochemical characterization, photostability, and antioxidant effects*. Anandam, S. and Selvamuthukumar, S., copyright (2014)



quercetin thermogram displayed a sharp endothermic peak at 318 °C (melting point of quercetin). Thermograms of NS were exhibited exothermic peaks nearby 350 °C. Similarly, the quercetin NS complex also displayed a broad exotherm around 350 °C. The disappearance of the drug endotherm was checked in the formulations prepared by freeze-drying. This showed proof of interactions between the polymer, crosslinker and active molecule, resulting in loss of crystal structure of drug as well as inclusion complex formation [28].

Thermal analysis of the plain meloxicam and meloxicam-loaded NS were examined. Thermogram of meloxicam presented peak at 250 °C which was found disappeared in thermogram of drug loaded NS, supporting the complexation between meloxicam and NS and protection of encapsulated drug in NS. The variation in the thermograms due to complexation and increase in the amorphization percentage of the drug NS complex indicated the dispersion of meloxicam in the hyper cross-linked colloidal structures [40]. A vast number of investigations employing DSC as one of the characterization approach is cited for camptothecin [33], resveratrol [24], paclitaxel [29], acetyl salicylic acid [25], gamma-oryzanol [82], telmisartan [26], curcumin [11], babchi oil [13] in various literature reports.

Thermogravimetric analysis

Thermal methods like TGA and DSC can be applied to empathize the holistic picture of true entrapment. In combination with DSC analysis, TGA of NS is often exploited to help and support the calculation of DSC observations. TGA measures the alteration in weight of sample on heating [1, 33]. The comparison of thermogravimetric curves of moieties and their NS formulations should be taken into account for ascertaining variations in the weight loss chart of NS matrix, witness of cross-linking between moieties and/or NS formulations. Thermogravimetry curves of both amorphous and crystalline polymers used in synthesis of NS, are mostly evaluated through difference in weight losses. In addition to this, it is evidenced that drug loaded NS should have different thermogravimetric behaviour from that of free drug due to increase in thermal stability [83].

To support the DSC studies, TGA curves of dexamethasone NS have also been explored. These curves exhibited that disappearance of endotherms of the pure drug in drug loaded NS, confirming the potential entrapment of active molecule in nanostructures [10].

Anandam and Selvamuthukumar synthesized nanosponges using β -cyclodextrin (polymer) and diphenyl carbonate (cross-linker) through microwave irradiation

technique. The thermal stability of the designed NS has been revealed up to 325 °C through TGA [15].

Thermo gravimetric analysis of blank NS, polyphenols and their NS complexes confirmed the physical mixture and inclusion complex of bioactives and NS. The first weight loss of the true polyphenol occurred at 109.5 °C, correlating its melting process as per standard specifications and again loss of weight appeared at 281.1 °C, indicating degradation process. Moreover, HMDI-NS (molar ratio 1:8) degraded after 315 °C and further, weight loss have been seen at 459.9 °C. From the NS thermal analysis results, it was declared that a slight change in peaks viz. 323.9, 336.2 and 461.3 °C, respectively, was observed in NS along with absence of free polyphenol. Similarly, in chlorogenic acid, a less profound peak at 214.1 °C and profound peak at 361.6 °C appeared. Rutin suffered weight loss at 110.3 °C followed by weight loss at 273.5 °C, corresponding to liquefying and degradation process, respectively. The degradation processes for all formulations have been observed from 280 to 331 °C, ascertaining their significant thermal stability [37].

Massaro and coworkers designed quercetin and silibinin (polyphenolic bioactive compounds) loaded NS by copolymerization of two supramolecular polymers β -CD and calix [4] arene in different molar ratios. The mass losses of the prepared NS with respect to the temperature change were depicted from the thermoanalytical curves. These curves indicated the thermal stability of the nanoformulations as well as the effect of the drug loading on the thermal stability. Both active molecules appeared to be degraded completely below 500 °C, but after encapsulation in NS, these molecules started weight loss from 500 °C. Further, it was evidenced that inclusion of quercetin and silibinin in the NS cavities modify the thermal stability of these molecules with a promise to enhance their thermal protection [84]. TGA as characterization tool for curcumin [49], and cholesterol [50], levodopa [43] is reported.

X-ray diffraction techniques

It is a useful and versatile nondestructive analytical technique to characterize and identify crystalline structures. It furnishes detailed information on texture, phases, structures and other structural parameters viz. crystallinity, average grain size, crystal defects and strain of molecules. It is established on the principle of constructive blocking of monochromatic X-rays and crystalline sample. The X-ray diffraction peak intensities are measured by dispersion of atoms in the lattice planes in the sample. Therefore, the X-ray diffraction is the fingerprint of periodic atomic systems in the examined sample [85]. Based on the nature of sample, this technique has been reported as single

crystal X-ray diffraction and PXRD. However, in most of the studies related to NS, PXRD has been reported. PXRD can be performed using homogenized sample to rapidly indentifying unknown crystalline material and to determine degree of crystallinity or amorphization of a sample. Unlike thermal analytical tools, the sample does not undergo any physical–chemical variation while spectrum recording and hence, can be reused for another analysis. Additionally, PXRD can be especially valuable to substantiate the measurements of thermal methods. In DSC investigation, minimization in magnitude or vanishing of melting peak of active moiety due to complete amorphization of the sample, can be validated by this technique.

First of all, drug encapsulation in NS can be proved from absence of respective drug peak in X-ray diffractograms. As seen in various NS formulations, this technique can confirm crystalline and amorphous nature of these nanosystems by detecting changes in 2θ values in comparison to physical mixtures, pure drug and NS. In addition, changes in intensity of diffractogram peaks gives an idea regarding crystalline size of NS. Crystalline and paracrystalline nature of nanosponges consequently affect solubility of these formulations, which is a valuable property in pharmaceutical products. Another remarkable parameter which can be revealed using this technique is porosity. It has been observed in literature that lyophilisation process leads to loss of crystal nature of these formulations which can be confirmed by PXRD.

Through careful interpretation of PXRD studies, it was anticipated that improvement of solubility and dissolution in ternary complexes of itraconazole was due to decrease particle size, reduction of crystal nature of itraconazole, surfactant role of copolyvidonum, and improvement in wetting and hiding of itraconazole hydrophobic groups by NS. In this study, Swaminathan and his research group carried out PXRD of itraconazole, their physical mixture and its nanosponge. These studies have ascertained conversion of drug to form amorphous in ternary complex as observed from decreased peaks number and their diminished areas [81].

In the year 2010, PXRD studies of camptothecin (CAM)-loaded NS showed crystalline and paracrystalline nature of nanoformulations (Fig. 6). CAM loaded crystalline NS demonstrated a crystalline structure due to chemical interactions. This was confirmed from comparison of PXRD patterns of CAM, physical mixture (CAM and β -CD) and CAM loaded NS. Hence, it was authenticated that CAM complexation is not a result of mixing of ingredients but due to engineering of a new arranged phase. However, paracrystalline NS demonstrated different loading capacity as CAM loading takes place as mechanical composite instead of inclusion matrix whereas crystalline CAM-NS showed different diffractograms having precise reflections and acceptable peak ratio. Further, for lower CD/cross linker ratio, the crosslinking

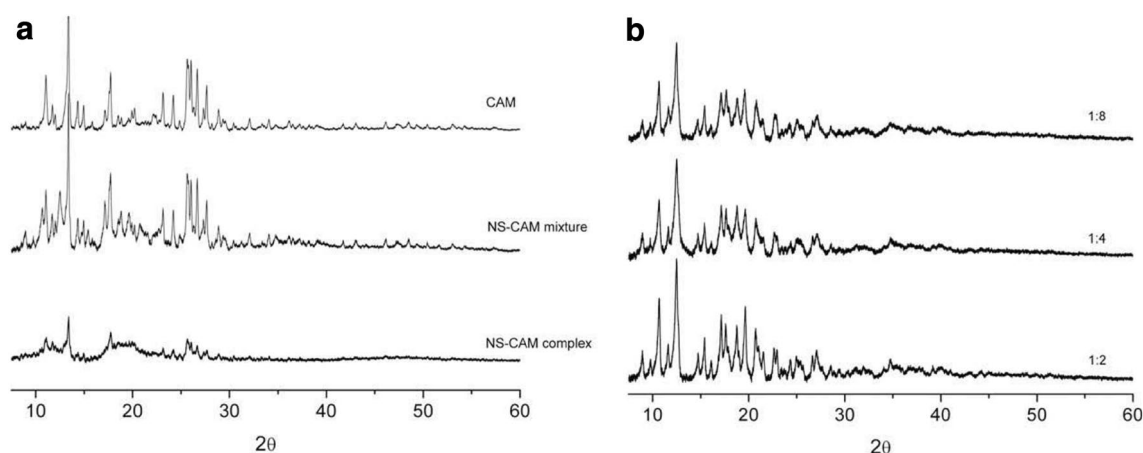


Fig. 6 **a** X-ray diagrams of crystalline CAM-loaded NSs (CAM–NS complex) compared with pure CAM–NS simulated physical mixture and plain CAM. **b** X-ray diagrams of crystalline NS at different b-CD/cross-linking agent ratio. Reprinted by permission from Elsevier: European Journal of Pharmaceutics and Biopharmaceutics,

Cyclodextrin-based nanospheres encapsulating camptothecin: Physicochemical characterization, stability and cytotoxicity. Swaminathan, S., Pastero, L., Serpe, L., Trotta, F., Vavia, P., Aquilano, D., Trotta, M., Zara, G., Cavalli, R, copyright (2010)

increases speedily whereas for translational and high values, it grows gradually [33].

Resveratrol, nanosponge complex and physical mixture were subjected to PXRD studies using simultaneous Bragg–Brentano geometry with sequential collection from 2.5° to 100° (2θ). The change in percentage crystallinity of nanospheres indicated resveratrol amorphization due to inclusion and/or non-inclusion of pure drug in NS. The enhanced resveratrol intensity was observed in comparison to intensity of drug in physical mixture and NS complex. The physical mixture and complex presented remarkable variations in the powder intensities and 2θ values. Further, the PXRD of lyophilized product depicted highly porous NS having amorphous nature [24].

In order to compare carbamate and carbonate polyphenol NS (fabricated from 1,1'-carbonyldiimidazole and hexamethylene diisocyanate crosslinkers, respectively) crystallinity, PXRD study was carried out. Both NS displayed paracrystalline structure which as confirmed through decomposition of some broad reflections in the diffractograms. Areas and intensity per FWHM (Full Width at Half Maximum) ratio were found variable, however a similar pattern of diffractogram was exhibited proving similar crystallinity in both NS designed from different crosslinkers [37].

A comparison of X-ray diffraction patterns of pure meloxicam with nanosponge formulations disclosed remarkable changes in the loss of crystallinity of the drug. The main peaks of meloxicam were presented at 17.50, 24.50, 28.50, 140, 210 and 230° (2θ) whereas these characteristic peaks were found completely weakened in drug loaded NS [40]. A number of studies using PXRD studies for analysing guest moieties like acetyl salicylic acid [25], telmisartan [26], acyclovir [34], curcumin [11], dexamethasone [10],

gamma-oryzanol [82], quercetin [28, 44], melatonin [41], efavirenz [12], chrysin [45], rilpivirine HCl [46], cholesterol [50], Rilpivirine [51] are mentioned in literature.

Microscopic techniques

Reckon on the material, microscopy may be employed as an explicit imaging analytical tool for NS, providing not only the quantitative information, but also qualitative analysis with regard to their shape, size and aggregation. Electron microscopy is based on the principle of wave description of fast poignant electrons. Visible light possess wavelength between 400 to 700 nm, electrons rapidly moving to 10,000 keV with 0.012 nm wavelength. Optical microscopes have narrow magnification of about 10³ diameters, due to diffraction of light. Electron microscopes have their resolution and magnification confined around 10⁶ diameter due to chromatic and spherical aberrations. This section provides knowledge regarding the tool like SEM, TEM, AFM CLSM, that have been suitably used for the characterization of NS [86].

Scanning electron microscopy

It is capable of developing high resolution pictures of a sample surface. These images possess a unique three dimensional debut and are effective in investigation of the surface structure of the given sample. SEM images are based on surface processes and adept to figure bulky samples with preminent depth resulting in good 3D representation of sample structure. Additional advantage of SEM is that permits a high quantity of the sample to focus at one time.

Because of these advantages, SEM is one of the most commonly used methods in research these days. Yet, it is also expensive and needs a high sample conductivity and vacuum [87]. This technique is also widely used in solid state evaluation of NS. It further allows a deep investigation of topography views of the starting material and physical mixtures of these materials and “cross-linked mixtures” designed by various techniques of NS preparation. This analytical tool provides the topographical changes corresponding to the interaction between the drug, polymer and cross-linker. Figure 7 represents the morphology of blank cyclodextrin nanosponges (as composed of β -CD and DPC).

In order to support FTIR, DSC and PXRD analysis, this technique has been employed to elucidate the surface topography of drug and their nanoformulations prepared by different methods [88].

In 2011, Alongi and co-workers investigated the surface topography of polypropylene-nanosponges paired with or without 2-hydroxy-4(octyloxy)-benzophenone (UV stabilizer) using SEM. The obtained images represented homogeneous and fine dispersion of the nanocarriers within the polymer matrix [89].

SEM investigation of the surface morphology of blank NS and resveratrol loaded NS depicted their highly porous nature and a clump forming capacity when suspended in water, evidencing interaction between polymer (CD) and crosslinker (CDI) [24].

Rao and her research group evaluated the surface morphology of NS using SEM. For this, the samples were engineered by lightly dusting of NS on adhesive tape mounted on a sample holder and then sputtering with platinum to a thickness (10 Å) under an argon atmosphere to minimise the

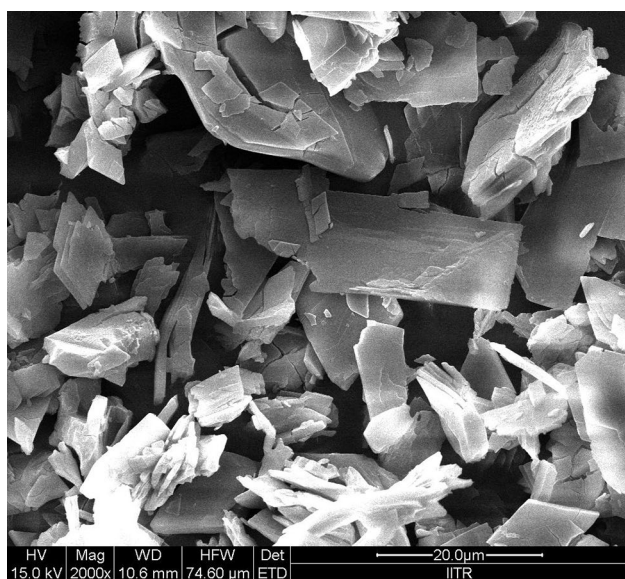


Fig. 7 FE-SEM images of blank crystalline β -CD nanosponges

charging effects. The stub having the coated samples was placed in the scanning electron microscope chamber. SEM of optimised telmisartan NS formulation, unencapsulated NS, polymer and pure drug were performed. SEM images represented prominent needle shaped crystals of the drug and porous NS [26].

Swaminathan et al, developed the samples of β -CD dexamethasone NS with ultrasound irradiation and without ultrasound irradiation. However, the SEM investigations, the difference lies in coating film which was gold film instead of platinum to overcome the charging burdens. The images showed crystalline morphologies for nanoformulation designed using ultrasound irradiation whereas disorganised structure was observed in other formulations prepared without ultrasound irradiation [10].

SEM images of meloxicam (MX) physical mixture (P), MX inclusion complex (K) and PMDA cross-linked MX nanosponges (N) showed that particle size of these formulations follow the order: $P > K > N$. The particle size of NS was observed 350 ± 5.69 nm smaller than MX molecules (particle size 2 μ m). The reduction in particle size of MX loaded NS indicated the significant encapsulation of drug, consequently resulting in solubility improvement [40].

SEM has also been carried out for various types of NS like babchi oil [13], curcumin [49], rosuvastatin [55], Sage essential oil [56].

Transmission electron microscopy

A nanoscale imaging tool, transmission electron microscopy may have resolution up to 0.2 nm [90, 91]. In this technique, a high voltage electron beam is transmitted through sample to create an image. To produce the electron beam, there are two types of sources: field-emission and thermionic. The field emitters are tungsten needles whereas thermionic ones are lanthanum hexaboride crystals and tungsten filaments [90]. This microscopic technique is relatively time consuming process with some time requiring extensive sample preparation. There is also possibility of sample damage by the electron beam. Although, an expensive analytical technique, it has been established as a promising tool to characterize and image various nanoparticles.

The TEM images of blank and camptothecin loaded NS prepared by melt method showed regular shape and size that remained as such after drug encapsulation. The average diameter of the plain paracrystalline NS (900 nm) was observed high in comparison to plain crystalline NS (400 nm). The mean particle size of the drug loaded paracrystalline and crystalline NS was measured 450 nm and 600 nm, respectively. Here in this research work, size was found slightly increased, in case of paracrystalline NS [33]. In another study, the suspension of the resveratrol NS was also characterized using TEM to ascertain their particle size

and shape. The images showed regular spherical morphology with size around 400 nm [24].

Mognetti and his research group evaluated particle size and shape of the paclitaxel loaded NS by TEM analysis. The drug incorporation was not found to affect the size and spherical topography of the NS in this work. Further, the TEM images of NS loaded fluorescein isothiocyanate dye showed uniform fluorescence, shape and size as that of unlabelled NS [29]. Similar results were reported for quercetin nanosponges [28].

In the following year, acyclovir loaded NS were found to have spherical shape and size around 400 nm with uniform distribution as depicted by TEM measurements [34]. High resolution transmission electron microscopy (HR-TEM) investigation of the bulk surface morphological characteristics of β -cyclodextrin dexamethasone nanosponges (both amorphous and crystalline) was carried out. The images depicted that crystalline β -cyclodextrin NS appeared as ordered structure with hexagonal symmetry and amorphous β -cyclodextrin NS as spherical shape, suggesting cross-linking between diphenyl carbonate and β -cyclodextrin [10].

From the TEM images, it was observed that the NS designed through microwave irradiation gave nearly spherical shape with uniform size distribution. The attributes of the crystal lattice in HR-TEM images were also measured at 0.70 nm [15].

In the following year, no effect on lemon grass oil NS integrity when incorporated into hydrogel was observed through TEM analysis [92].

Topography through TEM has also been carried out for various types of NS like actyl salicylic acid [25], zeolite [93], ibuprofen [67], chrysin [45] babchi oil [13], strigolactone [52], rosuvastatin [55], norfloxacin [48].

Atomic force microscopy

Recently advanced microscopic techniques with high resolution like AFM have been employed to view molecules and atoms with a few nanometres directly [94, 95]. This technique trusts on scanning of a nano-sized sharp probe on sample immobilized over a cautiously selected surface, like glass or mica, mounted on a piezoelectric scanner. AFM is equipped to minimise the basic limitations of scanning microscopy (only image semiconducting or conducting surfaces). The imaging of polymers, composites, glass, ceramics and biological samples can be done using AFM. Unlike, electron microscopy, AFM is reliable for imaging of biomolecules not only under physiological conditions but also during the biological process.

The detailed topography is not limited to crystalline sample due to high signal-to-noise ratio. Therefore, individual biomolecules, in absence of integral symmetry can be directly supervised in their native environment. The native

tissue, without prior dehydration can be analysed with AFM. The advantage of directly imaging molecular systems in their respective native environments affords the possibilities to examine their functional and structural properties at sub molecular level. AFM is unable to inspect the surface irregularities as observed through SEM. On the other hand when the tip is in direct touch with existent surface, it will go into problems because surface is sticky, soft or loses the molecules swimming on it.

In modern era, AFM images give the information on the topography of biomolecular systems, complementing other well established analytical methods like nuclear magnetic resonance (NMR), X-ray crystallography and, light and electron microscopy. AFM has been employed to figure molecular structure of β -cyclodextrin NS in the distilled water and examine their mechanical assets. The crystalline NS presented the spectacular crystal planes with ordinary height of nearby 500 nm whereas the paracrystalline NS exhibited spherical colloidal particles having average height of nearly 600 nm [10]. Morphology of the curcumin loaded NS was also elucidated through AFM [49].

Confocal laser scanning microscopy

It is an optical imaging proficiency for enhancing the optical contrast and resolution of a micrograph upon addition of a spatial pinhole fitted at the lens's confocal plane to annihilate out-of-focus light [96]. It is a sophisticated system of the optical electronic and mechanical components having advanced software for image acquisition. Initially, the CLSM enlighten the sample with lasers of different wavelength (from UV to infrared). The requirement of the laser is necessary to develop an intense beam that immediately focused down to a small spot (required for CSLM) [97].

Being the most versatile three dimensional imaging system, the CLSM have choice for both advanced and routine imaging applications. The CLSM is used to match the field of view with resolution using galvanometers to scan laser beam. In addition to this, it is also used to identify positive cell population and to count nuclei, when high resolution is not required. The CLSM also have excellent role in probing living cells with photobleaching and photoactivation [98, 99].

CLSM instrument takes more time (about 1 s) per image for 1024×1024 pixel image having $1 \mu\text{s}$ pixel dwell time. It leads to phototoxicity for live cell imaging because of the highly spatially and temporally localized laser spot. In spite of these limitations, CLSM is the good workhorse for life science research [96].

Lembo and his research group explored acyclovir loaded carboxylated NS for cellular uptake by CLSM. For this, fluorescent carboxylated NS were prepared. Growing Vero cells, plated and cultured in the 24-well plates were incubated in

10 μM of the fluoresceine isothiocyanate and washed with phosphate buffer solution for observing the living cells. The confocal sections under the fluorescent microscope revealed the cytoplasmic distribution of the fluorescent carboxylated NS after one h of its exposure to Vero cells. Hence, CLSM have promising application to detect the NS in the cells [34]. In another study, the 6-coumarin loaded β -cyclodextrin NS uptake in the PC-3 cells was also confirmed using CLSM [100].

Measurement of zeta potential and polydispersity indices

Scientifically, the zeta potential (ZP) is used for measuring the electrokinetic potential of the colloidal systems. Simply, ZP is the potential difference between the stationary layer of fluid to dispersion medium and dispersed particle. In other words, it is applicable to quantify the magnitude of the charge [101]. It can affect the phagocytosis of the nanoformulations as well as pharmacokinetic profile of the nanosystems in the body [102, 103]. To evaluate the charge conditions of the nanoparticles, the zeta potential should be measured by dispersing them in the original dispersion medium or distilled water [104].

The experimental techniques for the determination of the ZP are microelectrophoresis and electrophoretic light scattering [105]. This technique has been widely used in NS literature by various research groups. NS have been characterised through the electrophoretic light scattering method [26, 32, 42]. Practically, ZP allows predicting the sign of surface charge of the NS, followed by conditions for colloid stability. So, it cannot traverse especially in pharmaceutical products development.

Conclusion

The large growing interest towards nanosponges signifies their merits in pharmaceutical field. This is well established by the available literature and increasing the number of publications on this nanocarrier. The potential improvement in unfavorable chemical and physical properties of numerous active molecules through β -cyclodextrin nanosponges, along with their enhanced bioavailability at optimum cost has been widely reported. Analytical characterization of nanosponges, in liquid, solid and semisolid states represents a pivotal fundamental way to exploit the best potential of these nano carriers and further evaluate and broaden the possible applications of nanostructures. In fact, appropriate characterization can help significantly in choosing the most suitable polymer for formulating nanosponges having desired properties like, solubility and stability. Spectroscopic techniques, and

particularly FTIR, have played a fundamental role in confirmation of crosslinking of NS. Although reported in few studies, NMR can be extensively used for exploring the structural features of these colloidal carriers. Thermoanalytical techniques in combination with XRD endeavour a extensive supporting approach for extracting beneficial information corresponding to host–guest interactions and formation of NS. In addition, microscopic techniques like SEM and TEM can be adapted for an accurate analysis of size, shape and detailed morphology of NS. By incorporating fluorescent dye in NS, CLSM can be used to investigate their cytoplasmic distribution and mechanism of action in body cells. In order to evaluate stability of these systems, zeta potential and poly dispersity index measurement play a major role. Hence, these analytical techniques applied for characterization of nanosponges, when judiciously used are expected to furnish high-tech scientific explanations to this arena and arise with some prosperous products in pharmaceutical market in near future. Nanosponges have an arousing future, wherein it can provide site-directed drug delivery.

Acknowledgement The author, Sunil Kumar sincerely expresses gratitude to Indian Council of Medical Research, New Delhi for providing Senior Research Fellowship (Letter No: 45/44/2018-Nan/BMS).

Compliance with ethical standards

Conflict of interest The authors report no conflicts of interest in this work.

References

1. Trotta, F., Cavalli, R.: Characterization and applications of new hyper-cross-linked cyclodextrins. *Compos. Interface* **16**(1), 39–48 (2009)
2. Trotta, F., Zanetti, M., Cavalli, R.: Cyclodextrin-based nanosponges as drug carriers. *Beilstein J. Org. Chem.* **8**(1), 2091–2099 (2012)
3. David, F.: Nanosponge drug delivery system more effective than direct injection (2011)
4. Selvamuthukumar, S., Anandam, S., Krishnamoorthy, K., Rajappan, M.: Nanosponges: a novel class of drug delivery system-review. *J. Pharm. Pharm. Sci.* **15**(1), 103–111 (2012)
5. Ahmed, R.Z., Patil, G., Zaheer, Z.: Nanosponges—a completely new nano-horizon: pharmaceutical applications and recent advances. *Drug Dev. Ind. Pharm.* **39**(9), 1263–1272 (2013)
6. Li, D., Ma, M.: Cyclodextrin polymer separation materials. Patent WO, 9822197 (1998)
7. Trotta, F., Cavalli, R., Tumiatti, W., Zerbinati, O., Roggero, C., Vallero, R.: Ultrasound-assisted synthesis of cyclodextrin-based nanosponges. *WO2006002814 A1* (2006)
8. Trotta, F., Tumiatti, V., Cavalli, R., Roggero, C., Mognetti, B., Berta, G.: Cyclodextrin-based nanosponges as a vehicle for antitumoral drugs. WO, 3656, p. A1 (2009)
9. Trotta, F., Shende, P., Biasizzo, M.: Method for preparing dextrin nanosponges. WO2012147069 A1 (2012)
10. Swaminathan, S., Vavia, P.R., Trotta, F., Cavalli, R., Tumbiolo, S., Bertinetti, L., Coluccia, S.: Structural evidence of differential

- forms of nanosponges of beta-cyclodextrin and its effect on solubilization of a model drug. *J. Incl. Phenom. Macrocycl. Chem.* **76**(1–2), 201–211 (2013)
11. Darandale, S.S., Vavia, P.R.: Cyclodextrin-based nanosponges of curcumin: formulation and physicochemical characterization. *J. Incl. Phenom. Macrocycl. Chem.* **75**(3–4), 315–322 (2013)
 12. Rao, M.R., Shirsath, C.: Enhancement of bioavailability of non-nucleoside reverse transcriptase inhibitor using nanosponges. *AAPS PharmSciTech* **18**(5), 1728–1738 (2017)
 13. Kumar, S., Pooja, S., Trotta, F., Rao, R.: Encapsulation of babchi oil in cyclodextrin-based nanosponges: physicochemical characterization, photodegradation, and in vitro cytotoxicity studies. *Pharmaceutics* **10**(4), 169 (2018). <https://doi.org/10.3390/pharmaceutics10040169>
 14. Sharma, R., Pathak, K.: Polymeric nanosponges as an alternative carrier for improved retention of econazole nitrate onto the skin through topical hydrogel formulation. *Pharm. Dev. Technol.* **16**(4), 367–376 (2011)
 15. Anandam, S., Selvamuthukumar, S.: Optimization of microwave-assisted synthesis of cyclodextrin nanosponges using response surface methodology. *J. Porous Mat.* **21**(6), 1015–1023 (2014)
 16. Swaminathan, S., Darandale, S., Vavia, P.R.: Drug delivery/bioavailability-nanosponge-aided drug delivery: a closer look. *Pharm. Formul. Qual.* **14**(5), 12–15 (2012)
 17. Shende, P., Kulkarni, Y.A., Gaud, R.S., Deshmukh, K., Cavalli, R., Trotta, F., Caldera, F.: Acute and repeated dose toxicity studies of different β -cyclodextrin-based nanosponge formulations. *J. Pharm. Sci.* **104**(5), 1856–1863 (2015)
 18. Chilajwar, S.V., Pednekar, P.P., Jadhav, K.R., Gupta, G.J., Kadam, V.J.: Cyclodextrin-based nanosponges: a propitious platform for enhancing drug delivery. *Exp. Opin. Drug Deliv.* **11**(1), 111–120 (2014)
 19. Tejashri, G., Amrita, B., Darshana, J.: Cyclodextrin based nanosponges for pharmaceutical use: a review. *Acta. Pharm.* **63**(3), 335–358 (2013)
 20. Sherje, A.P., Dravyakar, B.R., Kadam, D., Jadhav, M.: Cyclodextrin-based nanosponges: a critical review. *Carbohydr. Polym.* **173**, 37–49 (2017)
 21. Venuti, V., Rossi, B., Mele, A., Melone, L., Punta, C., Majolino, D., Masciovecchio, C., Caldera, F., Trotta, F.: Tuning structural parameters for the optimization of drug delivery performance of cyclodextrin-based nanosponges. *Expert Opin. Drug Deliv.* **14**(3), 331–340 (2016)
 22. Indira, B., Boliseti, S.S., Samrat, C., Reddy, S.M., Reddy, N.S.: Nanosponges: a new era in drug delivery: review. *J. Pharm. Res.* **5**(11), 5293–5296 (2012)
 23. Szejtli, J.: Cyclodextrins and Their Inclusion Complexes (Akademiai Kiado, Budapest, 1982); J. Szejtli, *Cyclodextrin Technology* (1988)
 24. Ansari, K.A., Vavia, P.R., Trotta, F., Cavalli, R.: Cyclodextrin-based nanosponges for delivery of resveratrol: in vitro characterisation, stability, cytotoxicity and permeation study. *AAPS PharmSciTech* **12**(1), 279–286 (2011)
 25. Shende, P.K., Trotta, F., Gaud, R.S., Deshmukh, K., Cavalli, R., Biasizzo, M.: Influence of different techniques on formulation and comparative characterization of inclusion complexes of ASA with β -cyclodextrin and inclusion complexes of ASA with PMDA cross-linked β -cyclodextrin nanosponges. *J. Incl. Phenom. Macrocycl. Chem.* **74**(1–4), 447–454 (2012)
 26. Rao, M., Bajaj, A., Khole, I., Munjapara, G., Trotta, F.: In vitro and in vivo evaluation of β -cyclodextrin-based nanosponges of telmisartan. *J. Incl. Phenom. Macrocycl. Chem.* **77**(1–4), 135–145 (2013)
 27. Olteanu, A.A., Arama, C.C., Radu, C., Mihaescu, C., Monciu, C.M.: Effect of β -cyclodextrins based nanosponges on the solubility of lipophilic pharmacological active substances (repaglinide). *J. Incl. Phenom. Macrocycl. Chem.* **80**(1–2), 17–24 (2014)
 28. Anandam, S., Selvamuthukumar, S.: Fabrication of cyclodextrin nanosponges for quercetin delivery: physicochemical characterization, photostability, and antioxidant effects. *J. Mater. Sci.* **49**(23), 8140–8153 (2014)
 29. Mognetti, B., Barberis, A., Marino, S., Berta, G., De Francia, S., Trotta, F., Cavalli, R.: *In vitro* enhancement of anticancer activity of paclitaxel by a Cremophor free cyclodextrin-based nanosponge formulation. *J. Incl. Phenom. Macrocycl. Chem.* **74**(1–4), 201–210 (2012)
 30. Bragagni, M., Maestrelli, F., Mura, P.: Physical chemical characterization of binary systems of prilocaine hydrochloride with triacetin- β -cyclodextrin. *J. Incl. Phenom. Macrocycl. Chem.* **68**(3–4), 437–445 (2010)
 31. Menezes, P.P., Serafini, M.R., Santana, B.V., Nunes, R.S., Quintans, L.J., Silva, G.F., Medeiros, I.A., Marchioro, M., Fraga, B.P., Santos, M.R., Araujo, A.A.: Solid-state β -cyclodextrin complexes containing geraniol. *Thermochim. Acta* **548**, 45–50 (2012)
 32. Cavalli, R., Trotta, F., Tumiatti, W.: Cyclodextrin-based nanosponges for drug delivery. *J. Incl. Phenom. Macrocycl. Chem.* **56**(1–2), 209–213 (2006)
 33. Swaminathan, S., Pastero, L., Serpe, L., Trotta, F., Vavia, P., Aquilano, D., Trotta, M., Zara, G., Cavalli, R.: Cyclodextrin-based nanosponges encapsulating camptothecin: physicochemical characterization, stability and cytotoxicity. *Eur. J. Pharm. Biopharm.* **74**(2), 193–201 (2010)
 34. Lembo, D., Swaminathan, S., Donalizio, M., Civra, A., Pastero, L., Aquilano, D., Vavia, P., Trotta, F., Cavalli, R.: Encapsulation of Acyclovir in new carboxylated cyclodextrin-based nanosponges improves the agent's antiviral efficacy. *Int. J. Pharm.* **443**(1), 262–272 (2013)
 35. Kazarian, S.G., Wray, P.S.: Applications of FTIR spectroscopic imaging in pharmaceutical science. In: Ozaki, Y. (ed.) *Raman, Infrared, and Near-Infrared Chemical Imaging*, pp. 185–204. Wiley Online Library, Hoboken (2010)
 36. Castiglione, F., Crupi, V., Majolino, D., Mele, A., Rossi, B., Trotta, F., Venuti, V.: Inside new materials: an experimental numerical approach for the structural elucidation of nanoporous cross-linked polymers. *J. Phys. Chem. B.* **116**(43), 13133–13140 (2012)
 37. Ramírez-Ambrosi, M., Caldera, F., Trotta, F., Berrueta, L.A., Gallo, B.: Encapsulation of apple polyphenols in β -CD nanosponges. *J. Incl. Phenom. Macrocycl. Chem.* **80**(1–2), 85–92 (2014)
 38. Castiglione, F., Crupi, V., Majolino, D., Mele, A., Melone, L., Panzeri, W., Punta, C., Rossi, B., Trotta, F., Venuti, V.: Gel-sol evolution of cyclodextrin-based nanosponges: role of the macrocycle size. *J. Incl. Phenom. Macrocycl. Chem.* **80**(1–2), 77–83 (2014)
 39. Rao, M.R., Bhingole, R.C.: Nanosponge-based pediatric-controlled release dry suspension of Gabapentin for reconstitution. *Drug Dev. Ind. Pharm.* **41**(12), 2029–2036 (2015)
 40. Shende, P.K., Gaud, R.S., Bakal, R., Patil, D.: Effect of inclusion complexation of meloxicam with β -cyclodextrin and β -cyclodextrin-based nanosponges on solubility, in vitro release and stability studies. *Colloids Surf. B.* **136**, 105–110 (2015)
 41. Mihailiasa, M., Caldera, F., Li, J., Peila, R., Ferri, A., Trotta, F.: Preparation of functionalized cotton fabrics by means of melatonin loaded β -cyclodextrin nanosponges. *Carbohydr. Polym.* **142**, 24–30 (2016)
 42. Deshmukh, K., Tanwar, Y.S., Sharma, S., Shende, P., Cavalli, R.: Functionalized nanosponges for controlled antibacterial and antihypocalcemic actions. *Biomed. Pharmacother.* **84**, 485–494 (2016)

43. Trotta, F., Caldera, F., Cavalli, R., Soster, M., Riedo, C., Biasizzo, M., Uccello Barretta, G., Balzano, F., Brunella, V.: Molecularly imprinted cyclodextrin nanosponges for the controlled delivery of L-DOPA: perspectives for the treatment of Parkinson's disease. *Expert Opin. Drug Deliv.* **13**(12), 1671–1680 (2016)
44. Singireddy, A., Subramanian, S.: Cyclodextrin nanosponges to enhance the dissolution profile of quercetin by inclusion complex formation. *Particul. Sci. Technol.* **34**(3), 341–346 (2016)
45. Sundararajan, M., Thomas, P.A., Venkadeswaran, K., Jegannathan, K., Geraldine, P.: Synthesis and characterization of chrysin-loaded β -cyclodextrin-based nanosponges to enhance in-vitro solubility, photostability, drug release, antioxidant effects and antitumor efficacy. *J. Nanosci. Nanotechnol.* **17**(12), 8742–8751 (2017)
46. Zainuddin, R., Zaheer, Z., Sangshetti, J.N., Momin, M.: Enhancement of oral bioavailability of anti-HIV drug rilpivirine HCl through nanosponge formulation. *Drug Dev. Ind. Pharm.* **43**(12), 2076–2084 (2017)
47. Coviello, V., Sartini, S., Quattrini, L., Baraldi, C., Gamberini, M.C., La Motta, C.: Cyclodextrin-based nanosponges for the targeted delivery of the anti-restenotic agent DB103: A novel opportunity for the local therapy of vessels wall subjected to percutaneous intervention. *Eur. J. Pharm. Biopharm.* **117**, 276–285 (2017)
48. Mendes, C., Meirelles, G.C., Barp, C.G., Assrey, J., Silva, M.A., Ponchel, G.: Cyclodextrin based nanosponge of norfloxacin: Intestinal permeation enhancement and improved antibacterial activity. *Carbohydr. Polym.* **195**, 586–592 (2018)
49. Pushpalatha, R., Selvamuthukumar, S., Kilimozhi, D.: Cross-linked, cyclodextrin-based nanosponges for curcumin delivery-physicochemical characterization, drug release, stability and cytotoxicity. *J. Drug Deliv. Sci. Technol.* **45**, 45–53 (2018)
50. Singh, P., Ren, X., Guo, T., Wu, L., Shakya, S., He, Y., Wang, C., Maharjan, A., Singh, V., Zhang, J.: Biofunctionalization of β -cyclodextrin nanosponges using cholesterol. *Carbohydr. Polym.* **190**, 23–30 (2018)
51. Rao, M.R., Chaudhari, J., Trotta, F., Caldera, F.: Investigation of cyclodextrin-based nanosponges for solubility and bioavailability enhancement of rilpivirine. *AAPS PharmSciTech* (2018). <https://doi.org/10.1208/s12249-018-1064-6>
52. Argenziano, M., Lombardi, C., Ferrara, B., Trotta, F., Caldera, F., Blangetti, M., Koltai, H., Kapulnik, Y., Yarden, R., Gigliotti, L., Dianzani, U.: Glutathione/pH-responsive nanosponges enhance strigolactone delivery to prostate cancer cells. *Oncotarget.* **9**(88), 35813–35829 (2018)
53. Mady, F.M., Ibrahim, M., Ragab, S.: Cyclodextrin-based nanosponge for improvement of solubility and oral bioavailability of Ellagic acid. *Pak. J. Pharm. Sci.* **31**(5 Supplement Special), 2069–2076 (2018)
54. Zidan, M.F., Ibrahim, H.M., Afouna, M.I., Ibrahim, E.A.: In vitro and in vivo evaluation of cyclodextrin-based nanosponges for enhancing oral bioavailability of atorvastatin calcium. *Ind. Pharm. Drug Dev.* (2018). <https://doi.org/10.1080/03639045.2018.1442844>
55. Gabr, M.M., Mortada, S.M., Sallam, M.A.: Carboxylate cross-linked cyclodextrin: a nanoporous scaffold for enhancement of rosuvastatin oral bioavailability. *Eur. J. Pharm. Sci.* **111**, 1–12 (2018). <https://doi.org/10.1016/j.ejps.2017.09.026>
56. Nait Bachir, Y., Nait Bachir, R., Hadj-Ziane-Zafour, A.: Nano-dispersions stabilized by β -cyclodextrin nanosponges: application for simultaneous enhancement of bioactivity and stability of sage essential oil. *Ind. Pharm. Drug Dev.* (2018). <https://doi.org/10.1080/03639045.2018.1542705>
57. Raman, C.V., Krishnan, K.S.: A new type of secondary radiation. *Nature* **121**, 501–502 (1928)
58. Franzen, L., Windbergs, M.: Applications of Raman spectroscopy in skin research—From skin physiology and diagnosis up to risk assessment and dermal drug delivery. *Adv. Drug Deliv. Rev.* **89**, 91–104 (2015)
59. Mura, P.: Analytical techniques for characterization of cyclodextrin complexes in the solid state: a review. *J. Pharm. Biomed. Anal.* **113**, 226–238 (2015)
60. Crupi, V., Fontana, A., Majolino, D., Mele, A., Melone, L., Punta, C., Rossi, B., Rossi, F., Trotta, F., Venuti, V.: Hydrogen-bond dynamics of water confined in cyclodextrin nanosponges hydrogel. *J. Incl. Phenom. Macrocycl. Chem.* **80**(1–2), 69–75 (2014)
61. Rossi, B., Venuti, V., D'Amico, F., Gessini, A., Castiglione, F., Mele, A., Punta, C., Melone, L., Crupi, V., Majolino, D., Trotta, F.: Water and polymer dynamics in a model polysaccharide hydrogel: the role of hydrophobic/hydrophilic balance. *Phys. Chem. Chem. Phys.* **17**(2), 963–971 (2015)
62. Shuker, S.B., Hajduk, P.J., Meadows, R.P., Fesik, S.W.: Discovering high-affinity ligands for proteins: SAR by NMR. *Science* **274**(5292), 1531 (1996)
63. Ibanez, E., Cifuentes, A.: New analytical techniques in food science. *Crit. Rev. Food Sci. Nutr.* **41**(6), 413–450 (2001)
64. Mistry, N., Ismail, I.M., Farrant, R.D., Liu, M., Nicholson, J.K., Lindon, J.C.: Impurity profiling in bulk pharmaceutical batches using 19 F NMR spectroscopy and distinction between monomeric and dimeric impurities by NMR-based diffusion measurements. *J. Pharm. Biomed. Anal.* **19**(3), 511–517 (1999)
65. Salem, A.A., Mossa, H.A., Barsoum, B.N.: Application of nuclear magnetic resonance spectroscopy for quantitative analysis of miconazole, metronidazole and sulfamethoxazole in pharmaceutical and urine samples. *J. Pharm. Biomed. Anal.* **41**(2), 654–661 (2006)
66. Reinscheid, U.M.: Direct determination of ciprofloxacin in admixtures with metronidazol and ampicillin by NMR. *J. Pharm. Biomed. Anal.* **40**(2), 447–449 (2006)
67. Ferro, M., Castiglione, F., Punta, C., Melone, L., Panzeri, W., Rossi, B., Trotta, F., Mele, A.: Anomalous diffusion of Ibuprofen in cyclodextrin nanosponge hydrogels: an HRMAS NMR study. *Beilstein J. Org. Chem.* **10**(1), 2715–2723 (2014)
68. Biliaderis, C.G.: Differential scanning calorimetry in food research—a review. *Food Chem.* **10**(4), 239–265 (1983)
69. Cammenga, H.K., Epple, M.: Basic principles of thermoanalytical techniques and their applications in preparative chemistry. *Angew. Chem. Int. Ed. Engl.* **34**(11), 1171–1187 (1995)
70. Chartoff, R.P., Turi, E.A.: *Thermal Characterization of Polymeric Materials*, vol. 1, p. 513. Academic Press, New York (1997)
71. Prime, R.B.: Thermosets. In: Turi, E.A. (ed.) *Thermal Characterization of Polymeric Materials*. Academic Press, San Diego (1997)
72. Bair, H.E.: Thermal analysis of additives in polymers. In: Turi, A. (ed.) *Thermal Characterization of Polymeric Materials*, vol. 2. Polytechnic University, New York (1997)
73. Gallagher, P.K.: *Thermal Characterization of Polymeric Materials*. Academic Press, San Diego (1997)
74. Wunderlich, B.: *Basics of Thermal Analysis. Thermal Analysis of Polymeric Materials*, pp. 71–188. Springer, Berlin (2005)
75. Riga, A., Collins, R.: Differential scanning calorimetry and differential thermal analysis. In: Meyer, R.A. (ed.) *Encyclopedia of Analytical Chemistry*. Wiley, Chichester (2000)
76. Chen, W., Yang, L.J., Ma, S.X., Yang, X.D., Fan, B.M., Lin, J.: Crassicauline A/ β -cyclodextrin host–guest system: preparation, characterization, inclusion mode, solubilization and stability. *Carbohydr. Polym.* **84**(4), 1321–1328 (2011)
77. Bettinetti, G., Mura, P., Faucci, M.T., Sorrenti, M., Setti, M.: Interaction of naproxen with noncrystalline acetyl β -and acetyl

- γ -cyclodextrins in the solid and liquid state. *Eur. J. Pharm. Sci.* **15**(1), 21–29 (2002)
78. Wang, D.W., Ouyang, C.B., Liu, Q., Yuan, H.L., Liu, X.H.: Inclusion of quinestron and 2, 6-di-O-methyl- β -cyclodextrin: preparation, characterization, and inclusion mode. *Carbohydr. Polym.* **93**(2), 753–760 (2013)
79. Sunder, A.: Controlled polymerization of glycidol for the synthesis of hyperbranched polyglycerols and polyether polyols with variable molecular architectures (Doctoral dissertation, Dissertation, Albert-Ludwigs-Universität Freiburg) (2000)
80. Seiler, M.: Hyperbranched polymers: phase behavior and new applications in the field of chemical engineering. *Fluid Phase Equilib.* **241**(1), 155–174 (2006)
81. Swaminathan, S., Vavia, P.R., Trotta, F., Torne, S.: Formulation of betacyclodextrin based nanosponges of itraconazole. *J. Incl. Phenom. Macrocycl. Chem.* **57**(1–4), 89–94 (2007)
82. Sapino, S., Carlotti, M.E., Cavalli, R., Ugazio, E., Berlier, G., Gastaldi, L., Morel, S.: Photochemical and antioxidant properties of gamma-oryzanol in beta-cyclodextrin-based nanosponges. *J. Incl. Phenom. Macrocycl. Chem.* **75**(1–2), 69–76 (2013)
83. Coats, A.W., Redfern, J.P.: Thermogravimetric analysis. A review. *Analyst.* **88**(1053), 906–924 (1963)
84. Massaro, M., Cinà, V., Labbozzetta, M., Lazzara, G., Meo, P.L., Poma, P., Riela, S., Noto, R.: Chemical and pharmaceutical evaluation of the relationship between triazole linkers and pore size on cyclodextrin-calixarene nanosponges used as carriers for natural drugs. *RSC Adv.* **6**(56), 50858–50866 (2016)
85. Bunaciu, A.A., Udriștioiu, E.G., Aboul-Enein, H.Y.: X-ray diffraction: instrumentation and applications. *Crit. Rev. Anal. Chem.* **45**(4), 289–299 (2015)
86. Luykx, D.M., Peters, R.J., van Ruth, S.M., Bouwmeester, H.: A review of analytical methods for the identification and characterization of nano delivery systems in food. *J. Agric. Food Chem.* **56**(18), 8231–8247 (2008)
87. Fraunhofer, W., Winter, G.: The use of asymmetrical flow field-flow fractionation in pharmaceuticals and biopharmaceuticals. *Eur. J. Pharmacol. Biopharmacol.* **58**(2), 369–383 (2004)
88. Maestrelli, F., Cecchi, M., Cirri, M., Capasso, G., Mennini, N., Mura, P.: Comparative study of oxaprozol complexation with natural and chemically-modified cyclodextrins in solution and in the solid state. *J. Incl. Phenom. Macrocycl. Chem.* **63**(1–2), 17–25 (2009)
89. Alongi, J., Poskovic, M., Frache, A., Trotta, F.: Role of β -cyclodextrin nanosponges in polypropylene photooxidation. *Carbohydr. Polym.* **86**(1), 127–135 (2011)
90. Williams, D.B., Carter, C.B.: *Transmission Electron Microscopy, A Textbook for Materials Science*. Plenum Press, New York (1996)
91. Wang, Z.L.: Transmission electron microscopy of shape-controlled nanocrystals and their assemblies. *J. Phys. Chem. B.* **104**, 1153–1175 (2000)
92. Aldawsari, H.M., Badr-Eldin, S.M., Labib, G.S., El-Kamel, A.H.: Design and formulation of a topical hydrogel integrating lemongrass-loaded nanosponges with an enhanced antifungal effect: in vitro/in vivo evaluation. *Int. J. Nanomed.* **10**, 893 (2015)
93. Astafan, A., Benghalem, M.A., Pouilloux, Y., Patarin, J., Bats, N., Bouchy, C., Daou, T.J., Pinard, L.: Particular properties of the coke formed on nanosponge BEA zeolite during ethanol-to-hydrocarbons transformation. *J. Catal.* **336**, 1–10 (2016)
94. Ruozi, B., Tosi, G., Forni, F., Fresta, M., Vandelli, M.A.: Atomic force microscopy and photon correlation spectroscopy: two techniques for rapid characterization of liposomes. *Eur. J. Pharm. Sci.* **25**(1), 81–89 (2005)
95. Edwards, K.A., Baeumner, A.J.: Analysis of liposomes. *Talanta* **68**(5), 1432–1441 (2006)
96. Jonkman, J., Brown, C.M.: Any way you slice it—a comparison of confocal microscopy techniques. *J. Biomol. Tech.* **26**(2), 54 (2015)
97. Hagen, N., Gao, L., Tkaczyk, T.S.: Quantitative sectioning and noise analysis for structured illumination microscopy. *Opt. Express* **20**(1), 403–413 (2012)
98. Lippincott-Schwartz, J., Altan-Bonnet, N., Patterson, G.H.: Photobleaching and photoactivation: following protein dynamics in living cells. *Nat. Cell Biol.* **5**, S7–S14 (2003)
99. Patterson, G.H.: Photoactivation and imaging of photoactivatable fluorescent proteins. *Protoc. Cell Biol. Curr.* (2008). <https://doi.org/10.1002/0471143030.cb2106s38>
100. Gigliotti, C.L., Minelli, R., Cavalli, R., Occhipinti, S., Barrera, G., Pizzimenti, S., Cappellano, G., Boggio, E., Conti, L., Fantozzi, R., Giovarelli, M.: In vitro and *in vivo* therapeutic evaluation of camptothecin-encapsulated β -cyclodextrin nanosponges in prostate cancer. *J. Biomed. Nanotechnol.* **12**(1), 114–127 (2016)
101. Kutscher, H.L., Chao, P., Deshmukh, M., Rajan, S.S., Singh, Y., Hu, P., Joseph, L.B., Stein, S., Laskin, D.L., Sinko, P.J.: Enhanced passive pulmonary targeting and retention of PEGylated rigid microparticles in rats. *Int. J. Pharm.* **402**(1), 64–71 (2010)
102. Jabr-Milane, L.S., van Vlerken, L.E., Yadav, S., Amiji, M.M.: Multi-functional nanocarriers to overcome tumor drug resistance. *Cancer Treat. Rev.* **34**(7), 592–602 (2008)
103. Huynh, N.T., Passirani, C., Saulnier, P., Benoit, J.P.: Lipid nanocapsules: a new platform for nanomedicine. *Int. J. Pharm.* **379**(2), 201–209 (2009)
104. Radomska-Soukharev, A.: Stability of lipid excipients in solid lipid nanoparticles. *Adv. Drug Deliv. Rev.* **59**(6), 411–418 (2007)
105. Kedar, U., Phutane, P., Shidhaye, S., Kadam, V.: Advances in polymeric micelles for drug delivery and tumor targeting. *Nanomed. Nanotech. Biol. Med.* **6**(6), 714–729 (2010)

Publisher's Note Springer Nature remains neutral with regard to jurisdictional claims in published maps and institutional affiliations.